TECHNICAL AUDIOLOGY

Report TA No. 97
September 1980

STATISTICAL ANALYSIS OF FRICATIVE SOUNDS

Åke Olofsson

Report TA No. 97
September 1980

STATISTICAL ANALYSIS OF FRICATIVE SOUNDS

Åke Olofsson

From the Department of Technical Audiology
Karolinska Institutet
KTH
S-100 44 STOCKHOLM, Sweden

Tel: 46-8-11 66 60

Karolinska Institutet
Technical Audiology
KTH, S-100 44 Stockholm
Sweden

Report TA97
September 1980

STATISTICAL ANALYSIS OF FRICATIVE SOUNDS

Åke Olofsson

ABSTRACT

This report describes the results of an investigation of the properties of some Swedish fricative sounds. The investigation included analysis of autocorrelations, spectra, amplitude densities and statistics of zerocrossings for original sounds as well as autocorrelations and spectra after infinite peak clipping. The results of frequency division of peak clipped sounds are also shown. The use of frequency division for use in a transposer is discussed.

This work was supported by the National Swedish Board for Technical Development.

Table of Contents

1 INTRODUCTION.

For many years researchers have dealt with the problem of utilizing residual hearing in a more efficient way than by using simple amplification. When the residuum is limited to the low frequency range various attempts have been made to recode high frequency sounds, as for instance fricative sounds, into the low frequency range.

One such coding amplifier is the transposer constructed by B. Johansson (1966). This amplifier has one amplifying channel for the low frequency sounds and one channel for recoded high frequency sounds. The first version of the transposer had a high pass filter for separation of the high frequency sounds and a modulator for moving the information down to the low frequency range. This principle was used in two body-worn hearing aids, Tp64 and Tp65. In a later version of the transposer called Tp72, manufactured by Oticon A/S in Denmark, a nonlinearity was used instead of the linear modulator.

Another method for recoding has been used by Guttman et al (1970) and by Kringlebotn (1975) and also by Dryselius and Arlinger (1979). They have chosen peak clipping and frequency division with the use of flip-flops.

Among many of the users of the transposer there exists a strong desire that the transposer should be buildt in a version that could be worn behind the ear. Before starting any construction work, however, there was a need for a thorough investigation of the properties of fricative sounds. The aim of this study was therefore to find the physical parameters which are important for the perception of fricative sounds, and then to find a method for proper recoding which could be implemented in a behind-the-ear hearing aid.

2 SPEECH MATERIAL.

Recordings were made of fricative sounds from five different speakers. The speakers were given the instruction to try to keep the sound constant for at least one second. The fricatives were voiceless /s/- and /f/-sounds, /sh/-sound (as in shilling) and /ch/-sound (as in church).

The recordings were lowpass filtered with a cutoff frequency of 10 kHz, AD-converted with a sampling rate of 40 kHz and stored in a computer.

3 CHARACTERISTICS OF ORIGINAL SOUNDS.

3.1 Autocorrelation function.

The autocorrelation function of an ergodic time discreet process can be estimated as

$$r(i) = 1/N \sum_{n=0}^{N-1} x(n)x(n-i) \qquad (3.1.1)$$

where x(n) is a realization of the process.
For computation of (3.1.1) a fast and efficient method developed by Rader (1970) was used.

Plots of the normalized autocorrelation functions for the different sounds are found in figures 1-4. As can be seen from these figures there are certain similarities between the same fricatives for different speakers. It is however impossible to recognize any property of the autocorrelation functions that will separate different fricative sounds from each other independent of speaker.

The autocorrelation functions have also been correlated with each other to see if the shape of the autocorrelation function could be used to separate different fricatives. This showed however not to be the case as the correlations were not consistently high within each fricative group and not consistlently low between different groups.

3.2 Power spectral density.

The power spectral density of a stochastic process is the Fourier transform of the autocorrelation function.
To obtain estimates of the spectral densities of the fricatives the estimated autocorrelations were multiplied by a Hanning-window and Fourier transformed using a FFT-algorithm. Plots of the spectral densities are found in figures 5-8. As can be seen, the frequencies of the maximum amplitude peaks are for /s/-sounds around 6-7 kHz, for /f/-sounds 3.5-4 kHz (for speaker 1, however, 6 kHz), for /sh/-sounds 1.5-3 kHz and for /ch/-sounds 3.5-4 kHz. It can also be noticed that /f/-sounds have an amplitude peak around 600 Hz and a dip around 1 kHz.

3.3 Amplitude density.

Estimations of the one-dimensional probability density functions were made from the stored records. These showed that the hypothesis that fricative sounds are realizations of gaussian processes is not contradicted. Examples of amplitude densities are found in figure 9.

3.4 Zerocrossing interval.

The statistics for the time intervals between zerocrossings have been measured. The interesting parameters are the density function of interval lenght and the correlation between succesive intervals.

If the original sound has zerocrossings at times

$$t = \tau_1, \tau_2, \ldots, \tau_n, \ldots \qquad \tau_1 < \tau_2 < \ldots < \tau_n < \ldots \qquad (3.4.1)$$

a new sequence I(n) can be defined so that

$$I(n) = \tau_{n+1} - \tau_n \qquad n = 1,2,\ldots \qquad (3.4.2)$$

This new sequence is then equal to the time interval between zerocrossings and can be analysed for amplitude density and autocorrelation.

Figures 10-13 shows density functions for the length of the time intervals between zerocrossings for the fricatives. The time intervals are given in samples. As the sampling rate is 40 kHz the sampling interval equals 25 μs. The figures show that the peak densities occur for /s/-sounds around 3 samples (75 μs), for /f/-sounds around 2-4 samples (50-100 μs), for /sh/-sounds around 4-7 samples (100-175 μs) (for speaker 5, however, 11 samples) and for /ch/-sounds around 4-6 samples (100-150 μs).

It is also obvious from the figures that /s/-sounds have low density of intervals with length more than 6-7 samples (150-175 μs) and that the corresponding limits for /f/-sounds,/sh/-sounds and /ch/-sounds are 12-13 samples (300-325 μs), 12-18 samples (300-450 μs) and 10-11 samples (250-275 μs) respectively. Although the number of analysed sounds are few the differences in the limits mentioned above strongly indicate that the density functions of the interval length could be used to separate /s/-sounds from other fricative sounds.
Table 1 gives the mean time and standard deviation for the intervals between zerocrossings together with the correlation between succesive intervals and the average number of zerocrossings per second. It can be seen that the correlation between the length of time intervals decays rather rapidly with increasing interval distance, especially for /f/-sounds and that /ch/-sounds show the highest correlation of the four fricative sounds for time intervals immediately following each other.

In general /s/-sounds have the shortest mean time between zerocrossings and /sh/-sounds the longest. The quotient of standard deviation to mean value is lower for /s/-sounds and /ch/-sounds than for /f/- and /sh/-sounds.

		mean (μs)	s.d. (μs)	Zero-crossings per sec.	Correlation between length of intervals Interval distance 1	2	3	4	5
/s/-sound	Sp1	66	24	15160	.13	.08	.03	.01	.02
	Sp2	83	25	12120	.21	.09	.03	.01	.02
	Sp3	75	26	13300	.18	.10	.06	.01	.00
	Sp4	73	23	13570	.11	.01	.03	.04	.01
	Sp5	68	20	14650	.13	.11	.07	.04	.01
/f/-sound	Sp1	77	42	13070	.02	-.01	.05	.03	.00
	Sp2	114	54	8800	.19	-.02	.01	.05	.00
	Sp3	82	48	12210	.14	.01	.02	.03	.01
	Sp4	85	50	11730	.16	.03	-.01	.02	.03
	Sp5	86	47	11630	.15	-.01	-.03	.07	.00
/sh/-sound	Sp1	142	86	7020	.25	-.09	.06	.05	-.02
	Sp2	126	49	7970	.30	.09	.07	.06	.04
	Sp3	175	30	5710	.02	.04	-.15	-.04	-.15
	Sp4	133	57	7530	.34	.15	.04	.04	.03
	Sp5	222	117	4500	.14	-.10	.08	-.04	-.01
/ch/-sound	Sp1	116	42	8610	.33	.21	.11	.06	.06
	Sp2	126	43	7920	.32	.17	.08	.04	.03
	Sp3	134	42	7440	.37	.21	.09	.03	.01
	Sp4	131	44	7640	.36	.19	.12	.07	.07
	Sp5	104	35	9605	.28	.11	.02	.01	.02

TABLE 1. Mean and standard deviation for the time between zerocrossings, the average number of zerocrossings per second and the correlations between succesive time intervals for the original sounds.

4 INFINITE PEAK CLIPPING.

The original sound records have been passed through a nonlinearity that gives the output signals

$$y(n) = 1 \quad \text{if } x(n) \geq 0$$
$$y(n) = -1 \quad \text{if } x(n) < 0 \qquad (4.1)$$

where x(n) is the input signal.
The autocorrelation functions and spectra were estimated and compared with those of the original sounds.

4.1 Autocorrelation function.

If a gaussian process is passed through the nonlinearity described above the autocorrelation function will be

$$r_y(\tau) = 2/\pi \arcsin \rho_x(\tau) \qquad (4.1.1)$$

where $\rho_x(\tau)$ is the normalized autocorrelation function of the original process.

When figures 14-17, which shows the autocorrelations of the nonlinearely transformed sounds, were compared with the autocorrelation functions of original sounds shown in figures 1-4 the relation (4.1.1) was confirmed. This means that the original fricative sounds are realizations of gaussian processes.

The same conclusion that was drawn regarding the original sounds can be drawn for the transformed sounds; there is no obvious property of the autocorrelation functions that could be used to separate different fricatives from each other.

4.2 Power spectral density.

The power spectral densities of the infinitely peak clipped sounds are shown in figures 18-21. When comparing with the power spectral densities of the original sounds, shown in figures 5-8, it is found that the fine structures of the spectra are kept.
The dynamic range of the curves in figures 18-21 has however decreased compared with the dynamic range of the corresponding curves of figures 5-8. If for instance the peaks at the frequencies 4 kHz and 6 kHz for speaker 1 and /s/-sound are compared it is found that the amplitude difference is 16 dB in figure 5 but only 13 dB in figure 18.

A listening test showed that the peak clipped sounds and the original sounds were perceived as almost identical.

5 SYNTHETIC FRICATIVES.

Starting from the density functions for the time intervals between zerocrossings, shown in figures 10-13, synthetic fricatives have been created.

These new sounds have identical density functions for the time intervals between zerocrossings as the original sounds, but the correlations between succesive intervals are zero.

Examples of autocorrelation functions, spectra and zerocrossing density functions for two sounds are found in figure 22. The spectrum curves should be compared with the corresponding spectra of figure 18, speaker 1, and figure 21, speaker 1. It can then be seen that the frequencies of the amplitude peaks in figure 22 corresponds to the spectral centre of gravity of the curve in figure 18 and the curve in figure 21, respectively. The reason of this can be understood if the autocorrelation curves, also shown in figure 22, are compared with the autocorrela-

tion curves of speaker 1 in figures 14 and 17. The curves in figure 22 looks like the curves in figures 14 and 17 multiplied with a time window with a total duration of one ms. This will cause a smoothing of the spectra that corresponds well with the ones shown in figure 22.

When the synthesized sounds are compared with the peak clipped original sounds in a listening test, it is found that they sound rather alike, although the former do not have the tiny variations that makes the latter sound natural.

The density functions in figure 22 are obviously the same as those in figure 10, speaker 1, and figure 13, speaker 1.

6 FREQUENCY DIVISION.

Given an ergodic gaussian process, X(t), with autocorrelation function $r_x(\tau)$, the mean value of the number of zerocrossings per time unit is given by

$$E\langle N_0\rangle = \langle -r_x''(0)/r_x(0)\rangle^{1/2}/\pi \qquad (6.1)$$

if $r_x''(0)$ exists (Bendat, 1958, page 127).
The existence of $r_x''(0)$ is guaranteed if the spectrum of X(t) decreases as $1/f^{3+\varepsilon}$ with increasing f ($\varepsilon>0$). Bendat estimated the standard deviation for N_0 to be in the order of $\sqrt{N_0}$ or greater.

If a gaussian process is transformed by the nonlinearity described by (4.1) and then frequency divided by flip-flops the new signal will obviously have a spectrum which is lower in frequency than the spectrum of the original signal. The problem of giving an analytical expression for the resulting spectra is, however, yet not solved. It is possible to derive expressions (see for instance McFadden,1958), but certain assumptions about the correlations between succesive time intervals then has to be done, which strongly limits the use of the results.

The recorded fricative sounds were transformed according to this principle. The division factor was chosen to be eight. The resulting autocorrelation functions and spectra are shown in figures 23-26 and 27-30 respectively. Each spectra have a marked peak and especially the /s/--sounds have steep sloopes around this peak. The peaks are located at somewhat higher frequencies for the /s/-sounds and the /f/-sounds than for the /sh/-sounds and the /ch/-sounds. If the curves for speaker 1 in figures 27 and 30 are compared with the spectra in figure 22 it can be seen that the spectral peaks of the synthetic sounds are located at frequencies approximately eigth times greater than the frequencies of the transposed sounds.

It can also be noticed that the relative bandwidth of the sounds have decreased.

7 CONCLUSIONS.

When the spectra of the original sounds (figures 5-8) were compared with the spectra of the peak clipped sounds (figures 18-21) it was found that the correspondance was indeed very good. As peak clipping obviously does not change the zerocrossings this means that no information about the original sound (except for an amplitude factor) is lost under peak clipping. Comparative listening tests also confirmed this.

When on the other hand the peak clipped sounds were compared with the synthetic sounds, described in chapter 5, listening tests showed that they sounded rather alike. It was also found that the spectra of the synthetic sounds were smoothed versions of the spectra of the peak clipped sounds. This indicates that the major parts of the information about the original sounds are contained in the one-dimensional density functions for the time between zerocrossings.

Frequency division of the peak clipped sounds were found to give spectra with peaks at frequencies one division factor below the frequencies of the peaks of the synthetic sounds. If the division factor is not chosen too large most of the zerocrossing information will also be kept. The total information contained in the peak clipped, frequency divided sounds is then roughly the same as the information contained in the synthetic sounds, but coded in another way.

The conclusion is then that peak clipping and frequency division might be a useful way to transpose high frequency fricative sounds into low frequency sounds, in such a way that the differences that exist between original sounds are mainly preserved.

8 REFERENCES.

Bendat J.S.(1958) Principles and Applications of Random Noise Theory. John Wiley & Son, New York.

Dryselius H. & Arlinger S. (1979) Frekvensbandskompression. Reports from Technical Audiology, Linköping University, Linköping, No. LiTA 79-3.

Guttman N., Levitt H. & Bellefleur P.A.(1970) Articulatory Training of the Deaf using Low-frequency Surrogate Fricatives. Journal of Speech and Hearing Research Vol 13,19-29.

Johansson B.(1966) The Use of the Transposer for the Management of the Deaf Child. International Audiologi Vol V No 3, 362-372.

Kringlebotn M. (1975) Oppfattelse av frekvensdividerte talelyder. Reports from ELAB, University of Trondheim, Trondheim, No. STF44 A75068.

McFadden J.A.(1958) The Axis-Crossing Intervals of Random Functions. IRE Trans. on Information Theory Vol IT-4,14-24.

Rader C.M. (1970) An Improved Algorithm for High Speed Autocorrelation with Application to Spectral Estimation. IEEE Trans. Audio Electroacoust. Vol AU-18, 439-441.

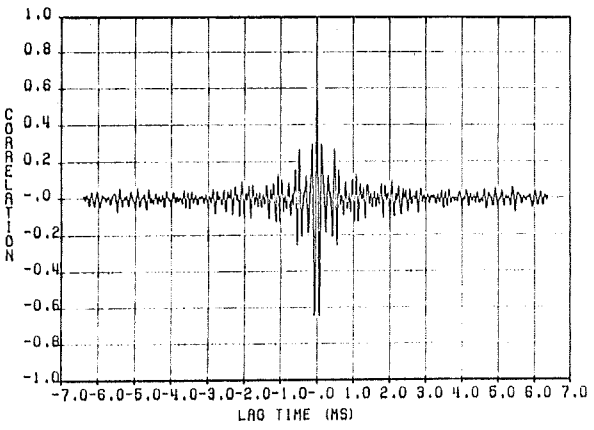

Speaker 1

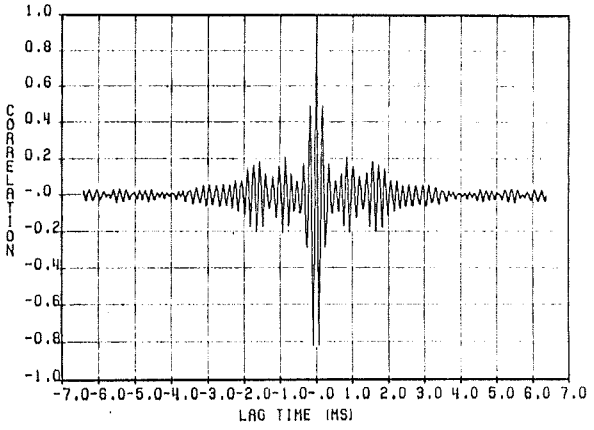

Speaker 2

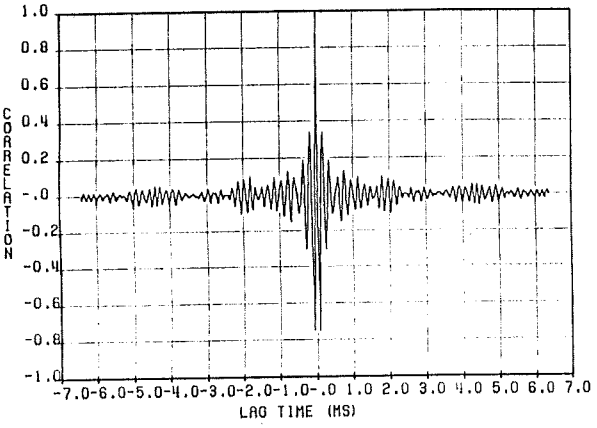

Speaker 3

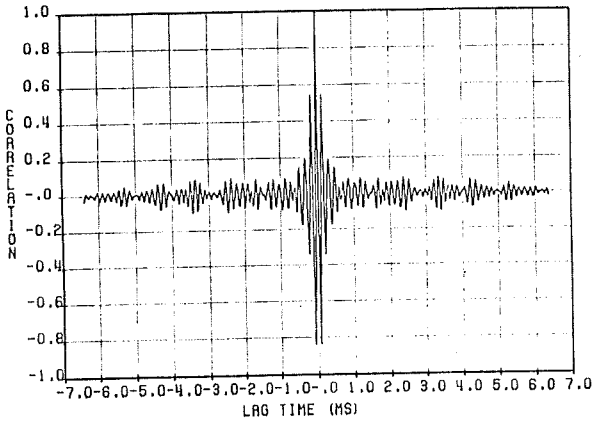

Speaker 4

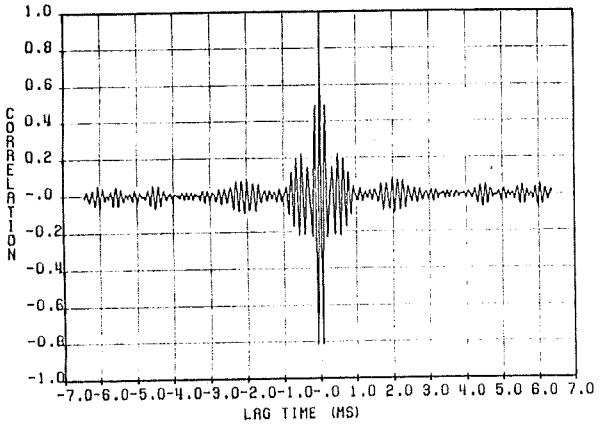

Speaker 5

FIGURE 1. Normalized autocorrelation functions for /s/-sounds.

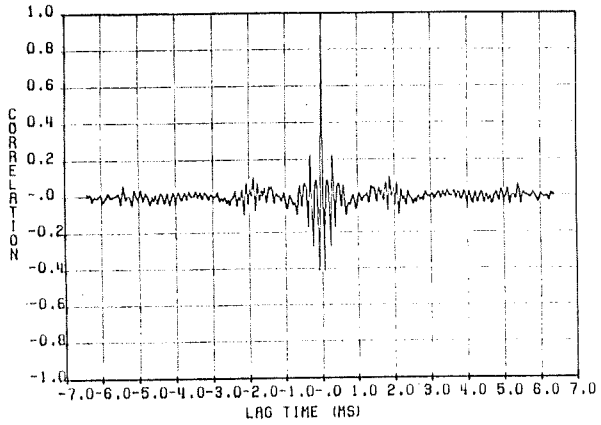

Speaker 1

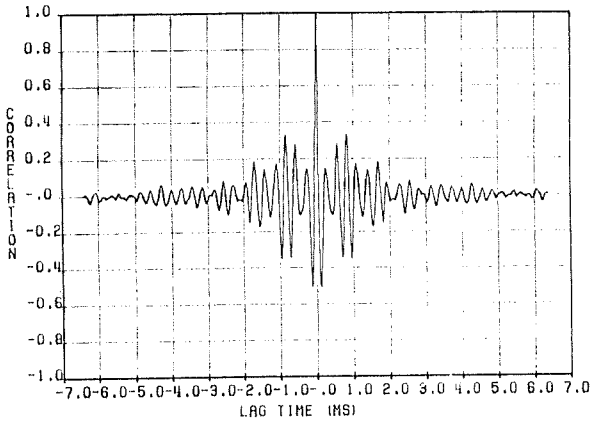

Speaker 2

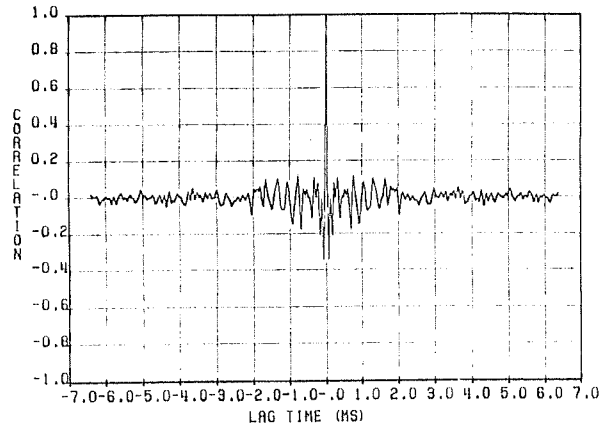

Speaker 3

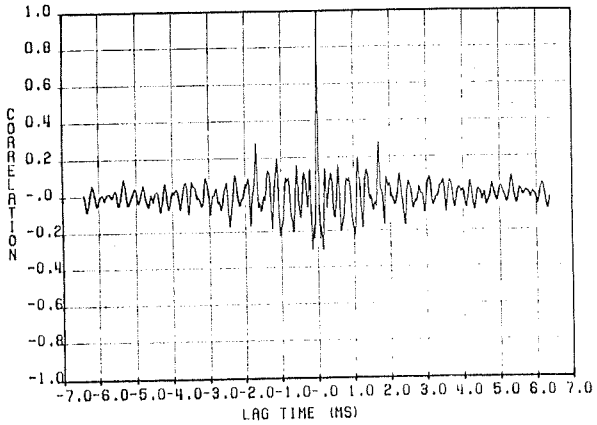

Speaker 4

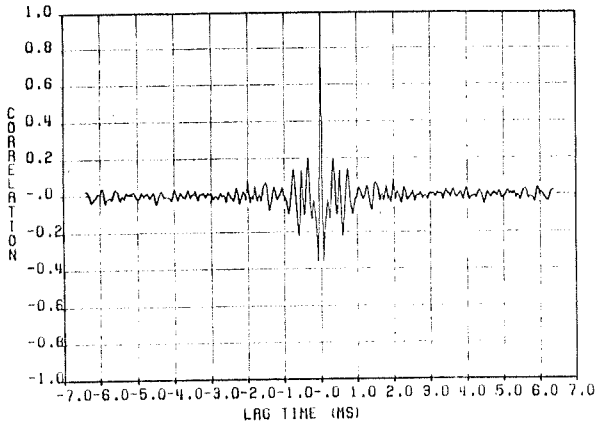

Speaker 5

FIGURE 2. Normalized autocorrelation functions for /f/-sounds.

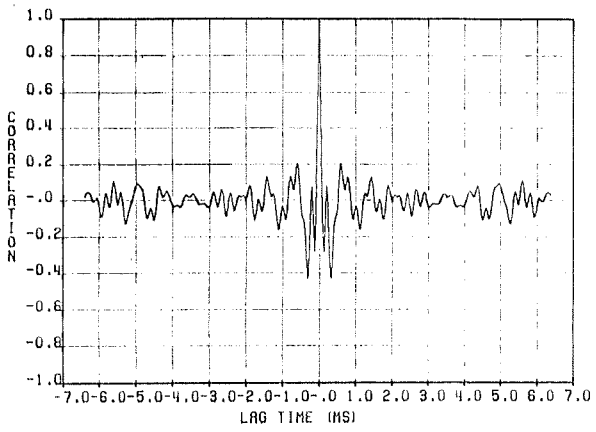

Speaker 1

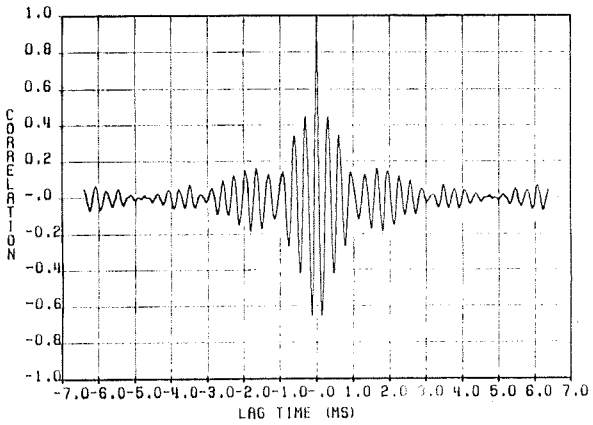

Speaker 2

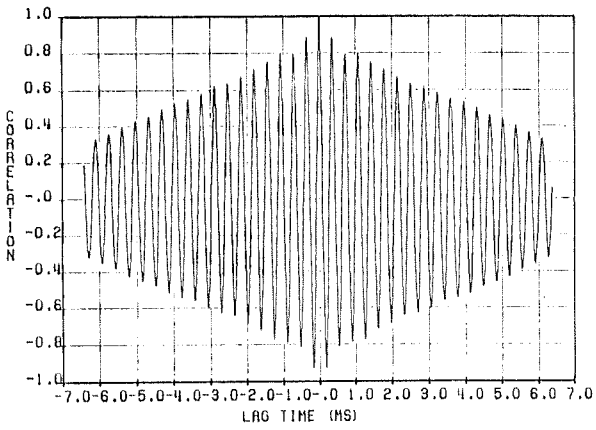

Speaker 3

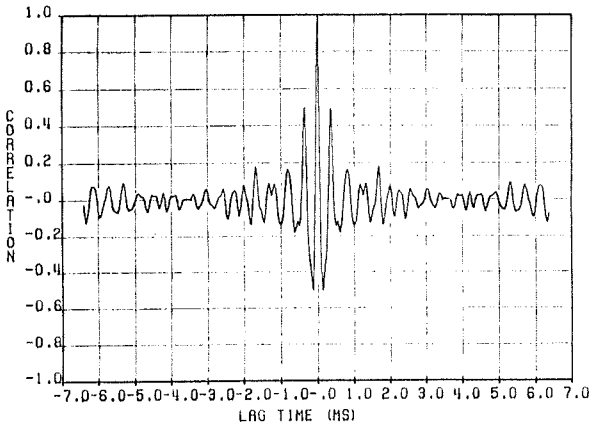

Speaker 4

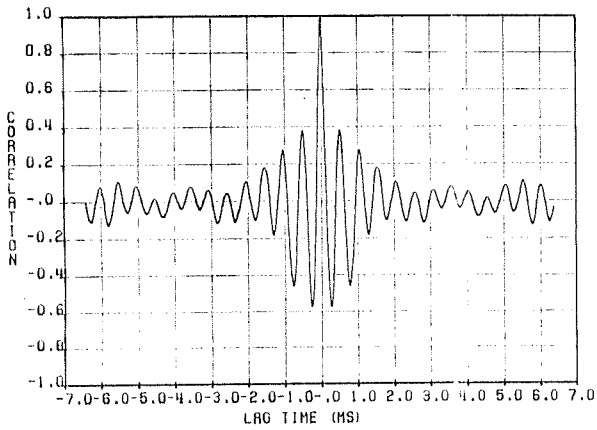

Speaker 5

FIGURE 3. Normalized autocorrelation functions for /sh/-sounds.

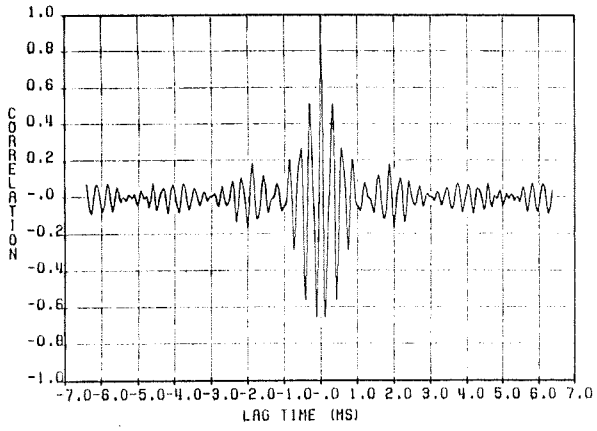

Speaker 1

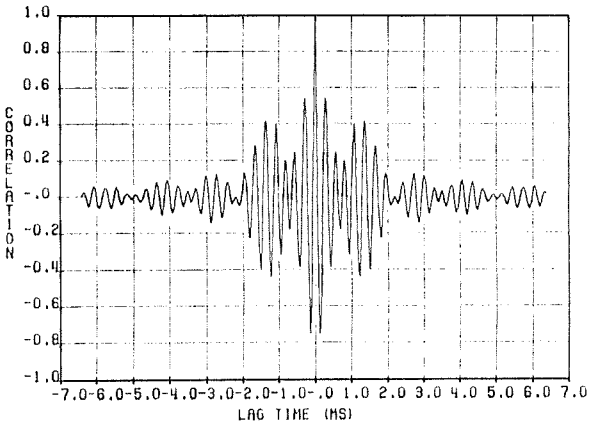

Speaker 2

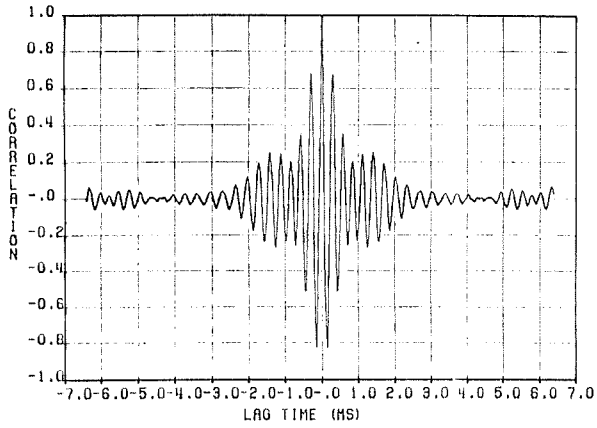

Speaker 3

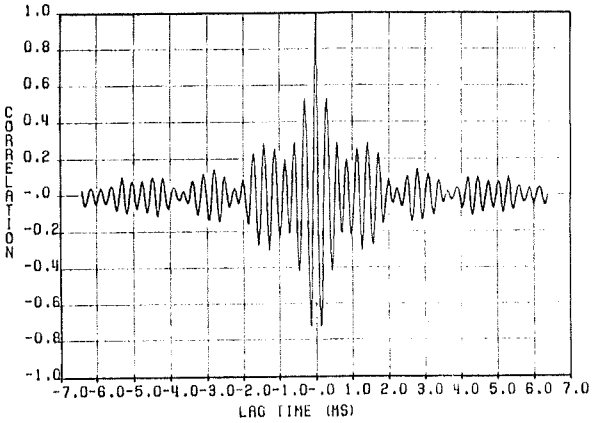

Speaker 4

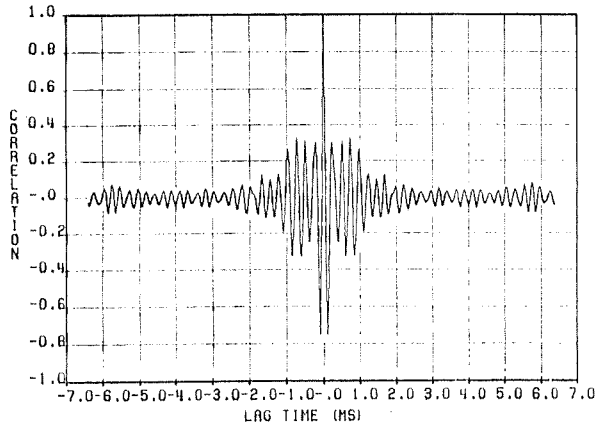

Speaker 5

FIGURE 4. Normalized autocorrelation functions for /ch/-sounds.

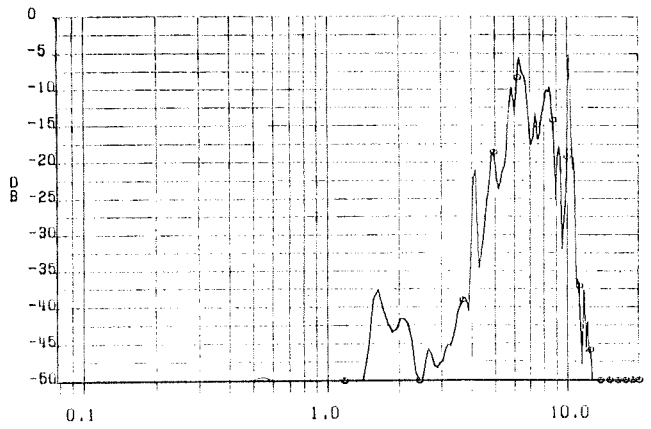

Speaker 1

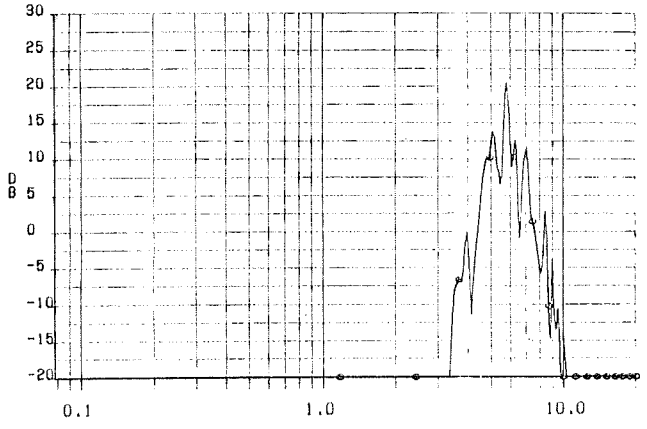

Speaker 2

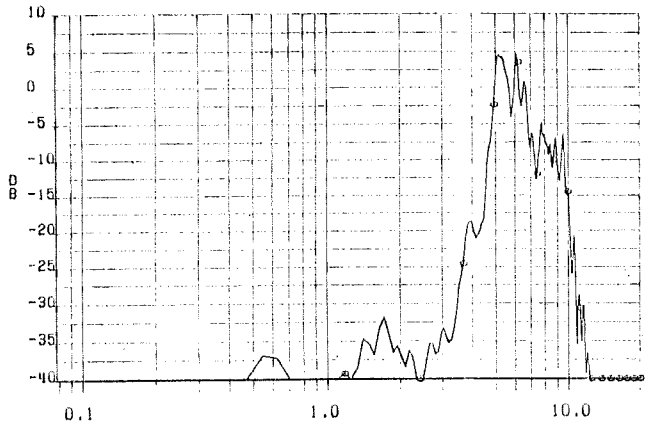

Speaker 3

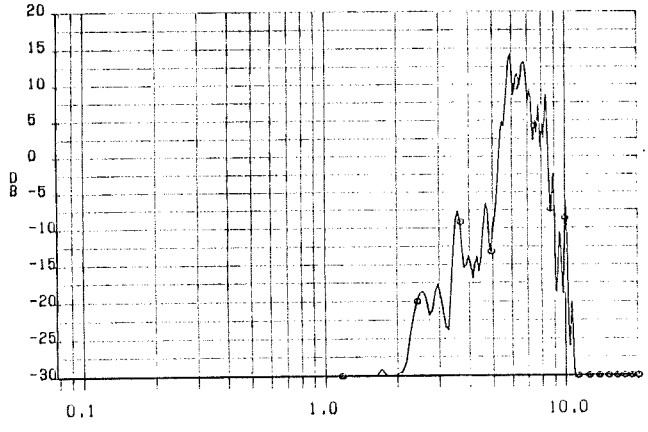

Speaker 4

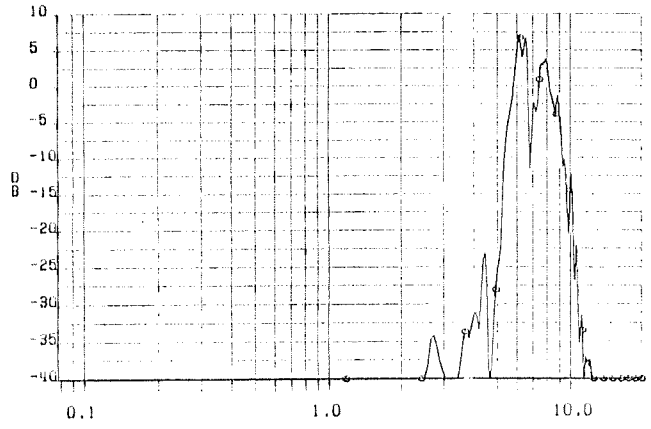

Speaker 5

FIGURE 5. Power spectral density functions for /s/-sounds.

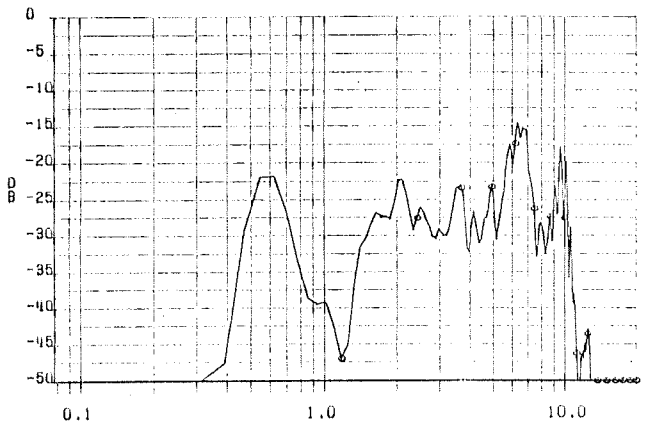

Speaker 1

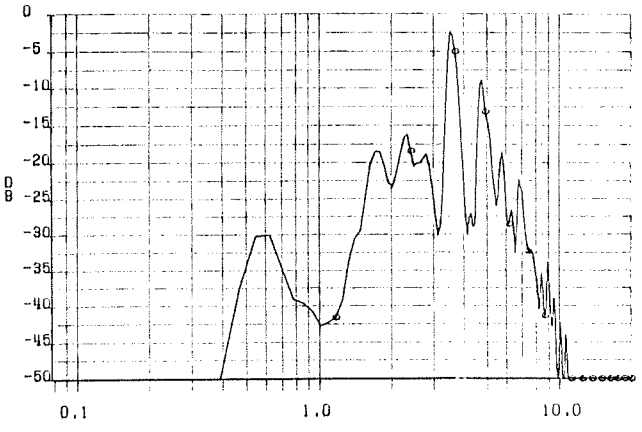

Speaker 2

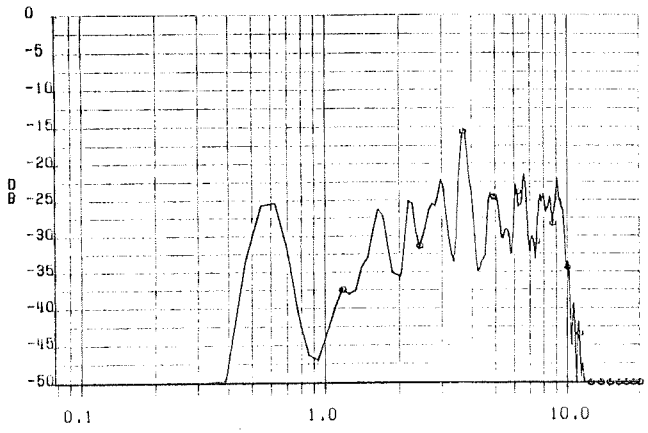

Speaker 3

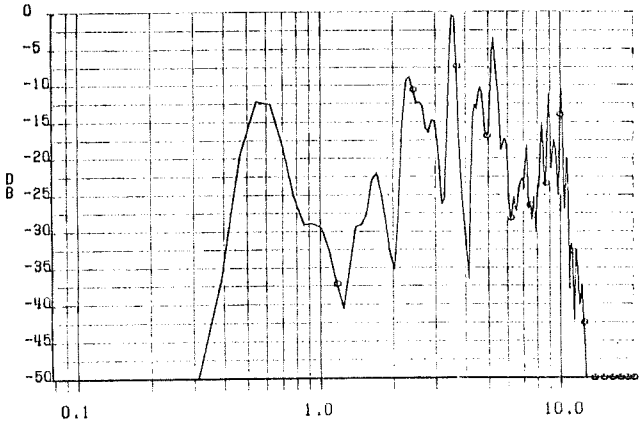

Speaker 4

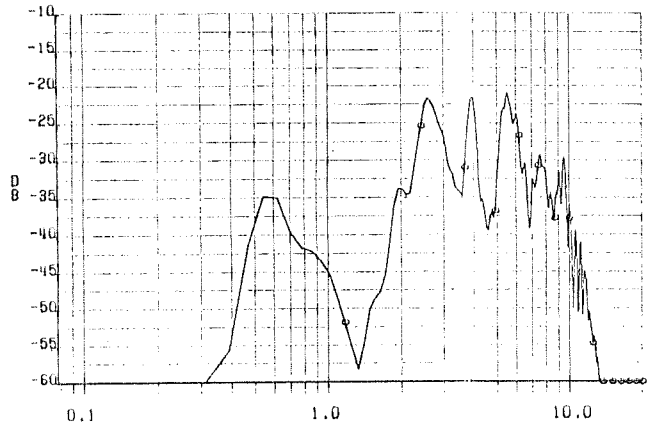

Speaker 5

FIGURE 6. Power spectral density functions for /f/-sounds.

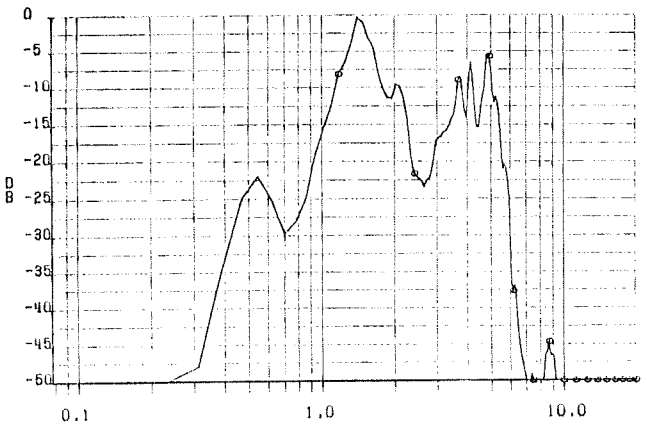

Speaker 1

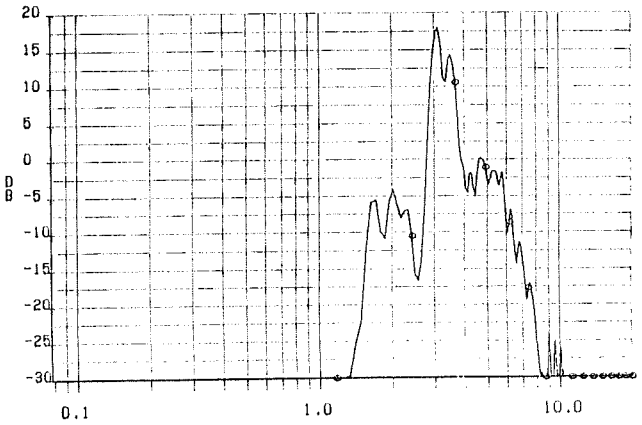

Speaker 2

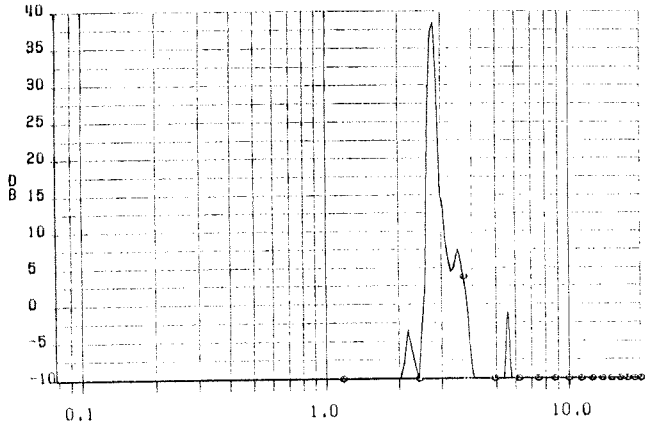

Speaker 3

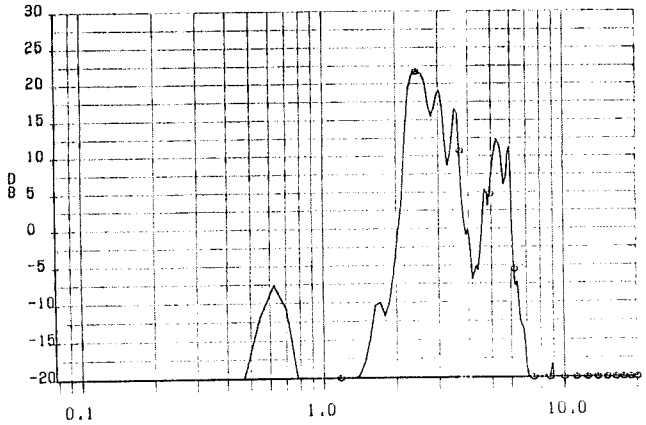

Speaker 4

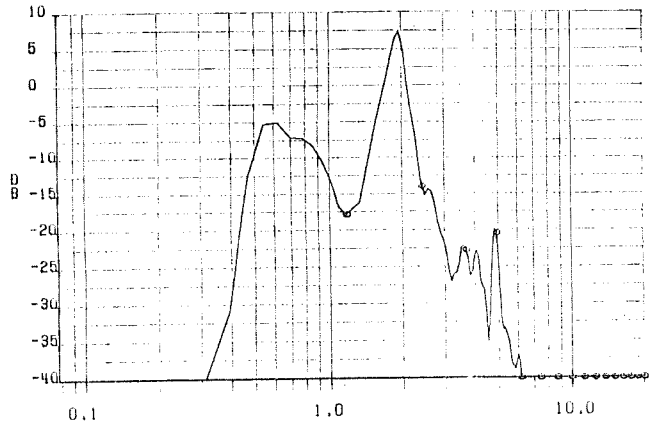

Speaker 5

FIGURE 7. Power spectral density functions for /sh/-sounds.

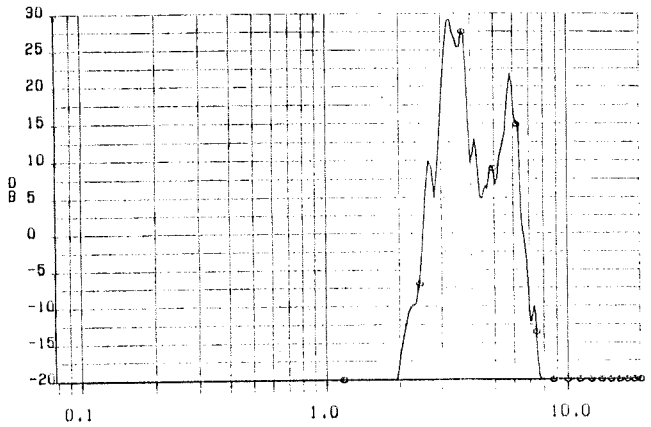

Speaker 1

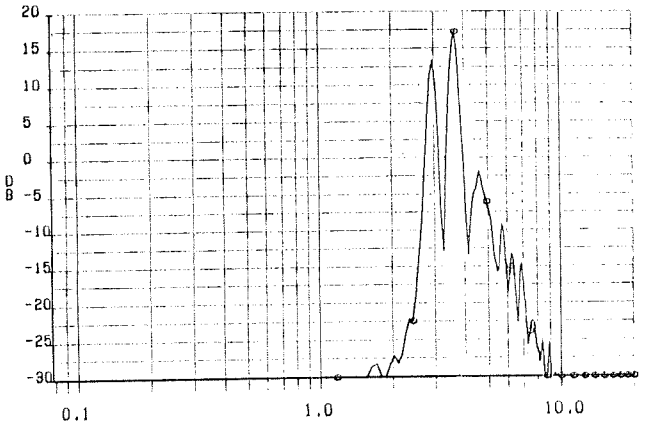

Speaker 2

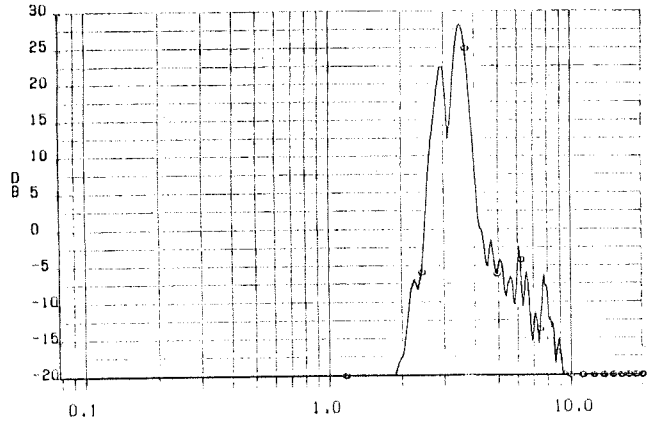

Speaker 3

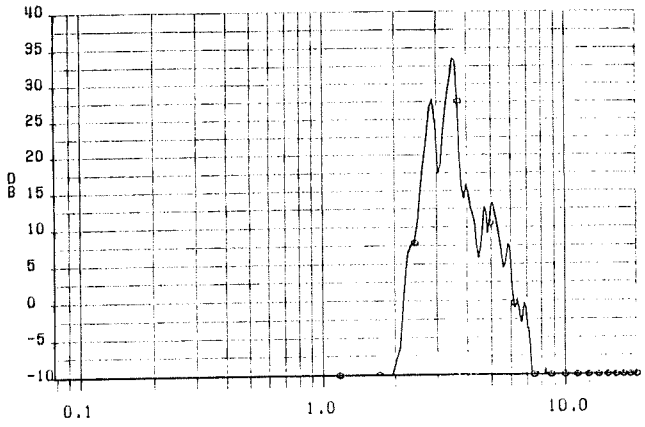

Speaker 4

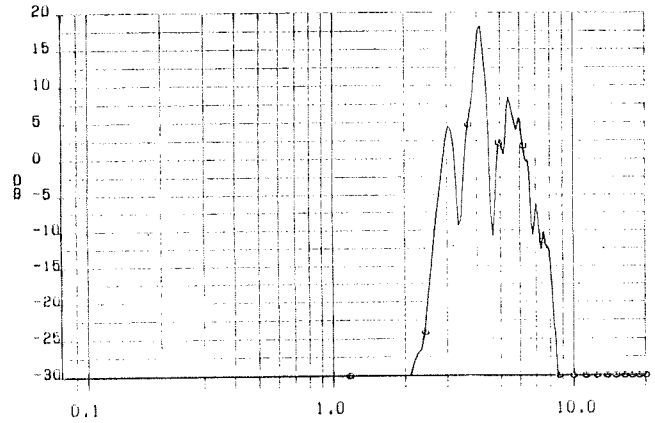

Speaker 5

FIGURE 8. Power spectral density functions for /ch/-sounds.

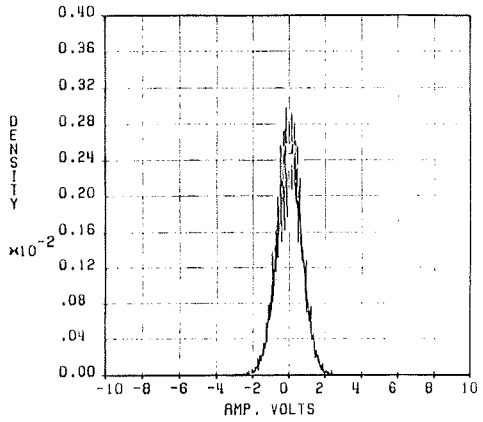

/s/-sound

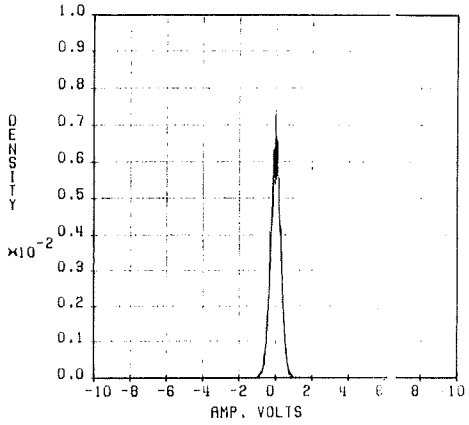

/f/-sound

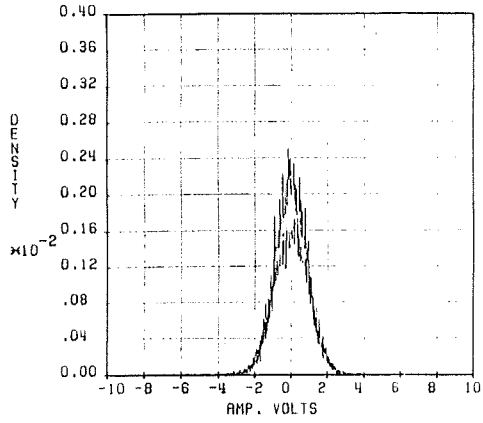

/sh/-sound

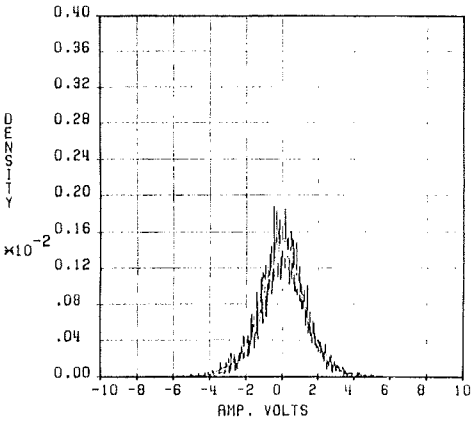

/ch/-sound

FIGURE 9. Amplitude density functions for speaker 4.

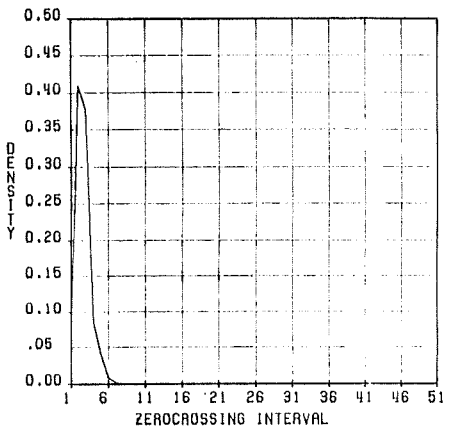

Speaker 1

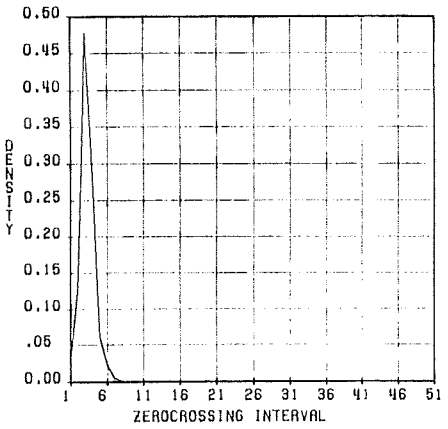

Speaker 2

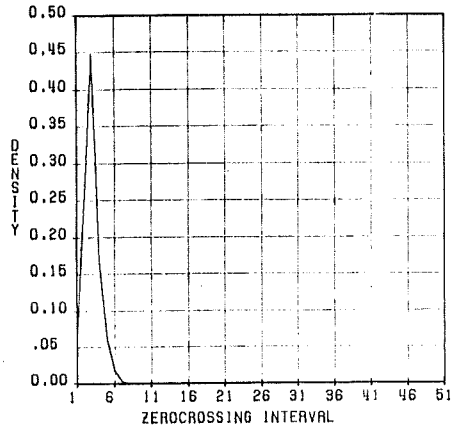

Speaker 3

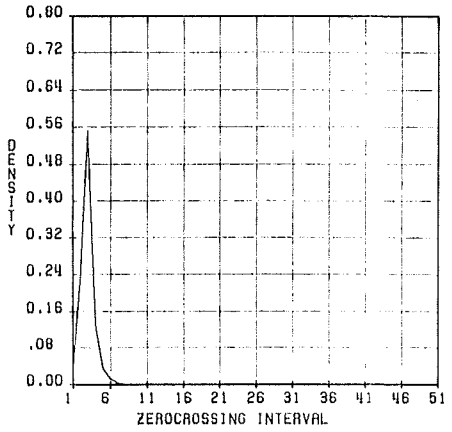

Speaker 4

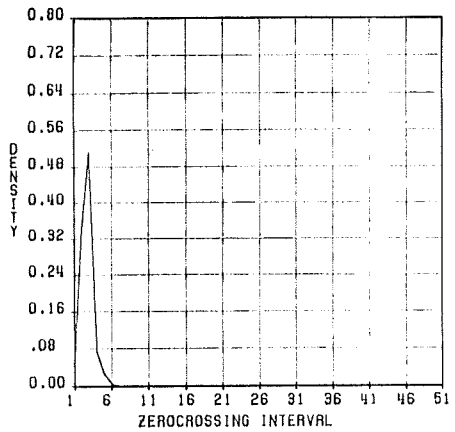

Speaker 5

FIGURE 10. Density functions for the time between zerocrossings for /s/-sounds.

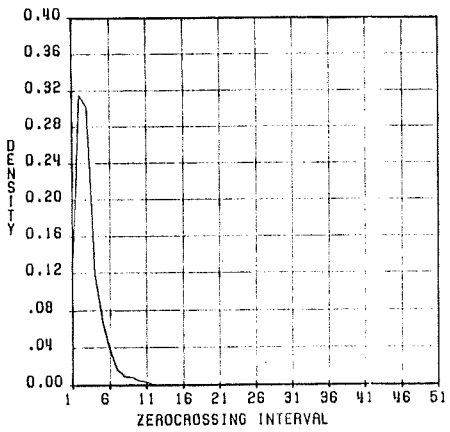

Speaker 1

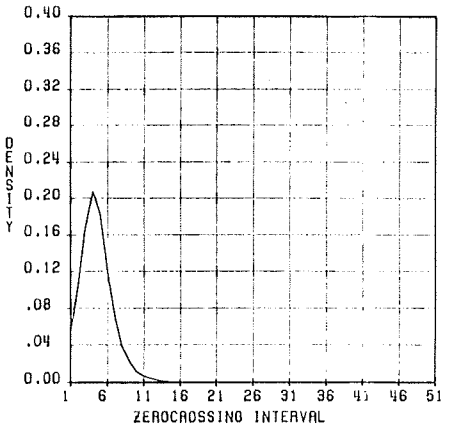

Speaker 2

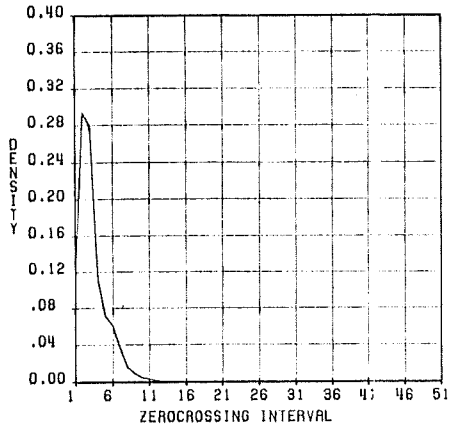

Speaker 3

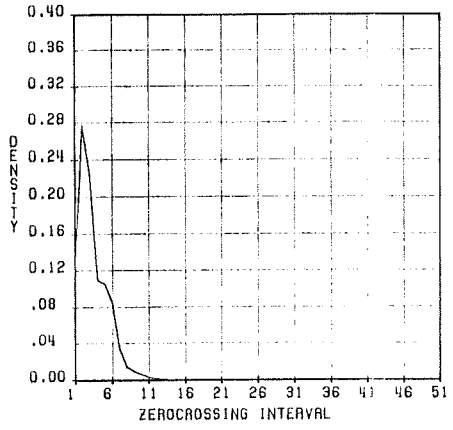

Speaker 4

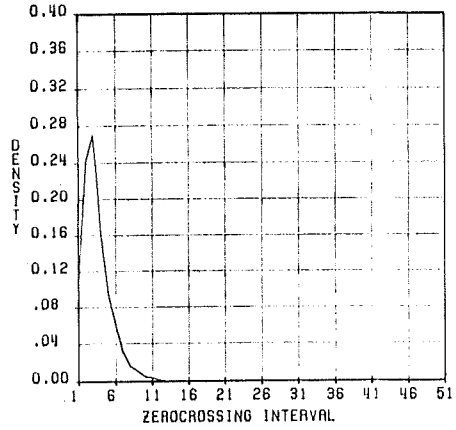

Speaker 5

FIGURE 11. Density functions for the time between zerocrossings for /f/-sounds.

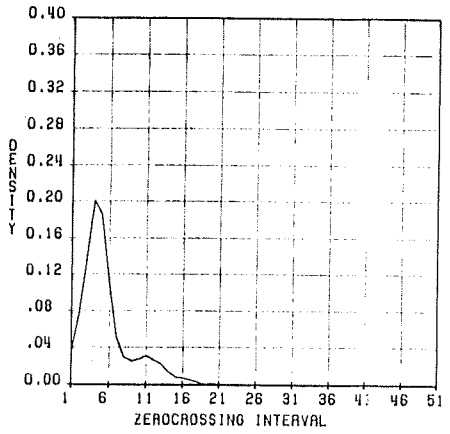

Speaker 1

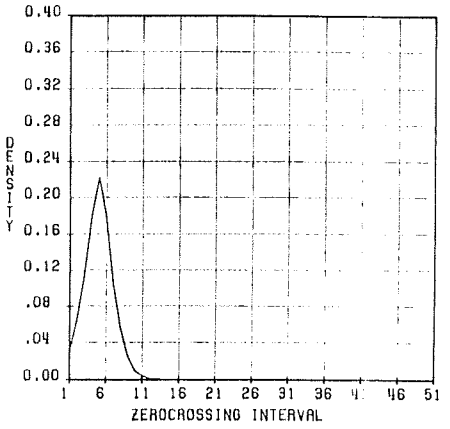

Speaker 2

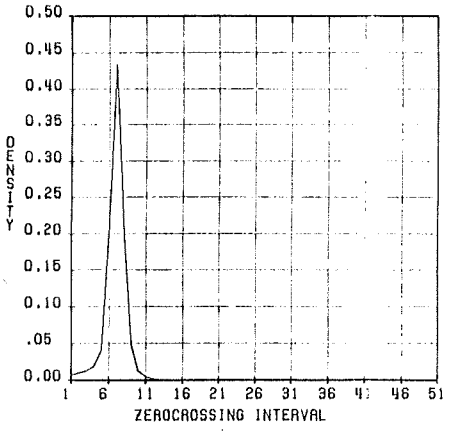

Speaker 3

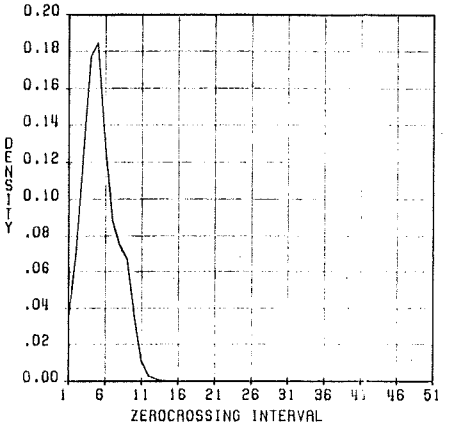

Speaker 4

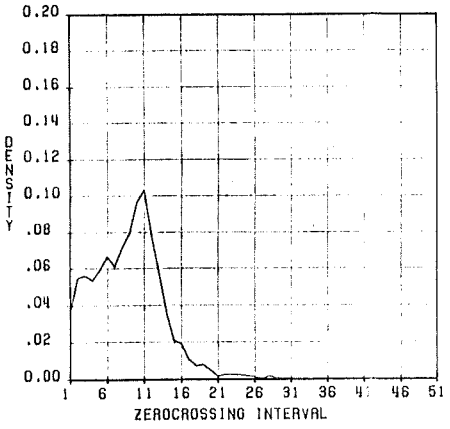

Speaker 5

FIGURE 12. Density functions for the time between zerocrossings for /sh/-sounds.

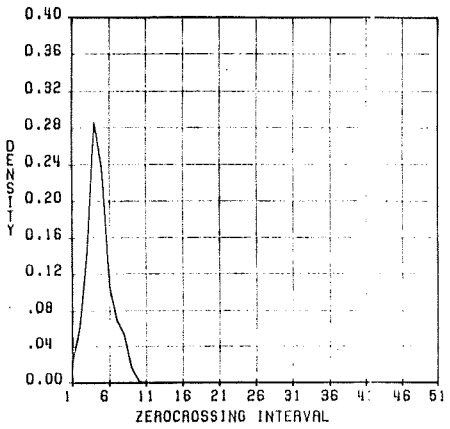

Speaker 1

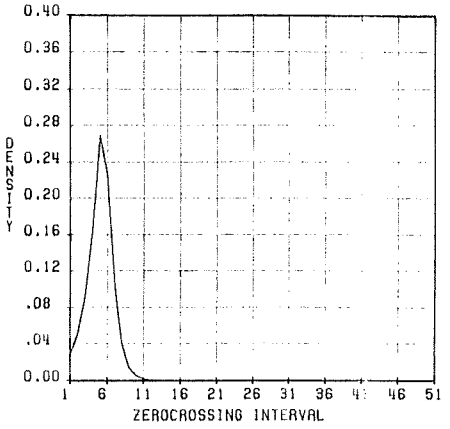

Speaker 2

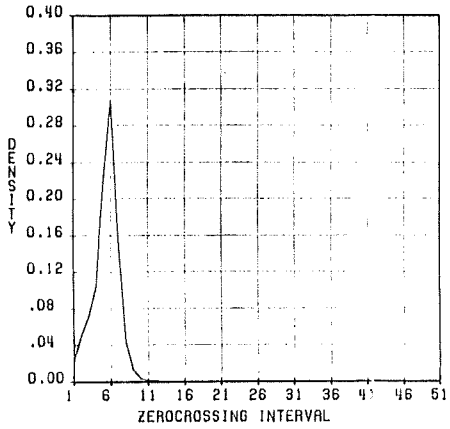

Speaker 3

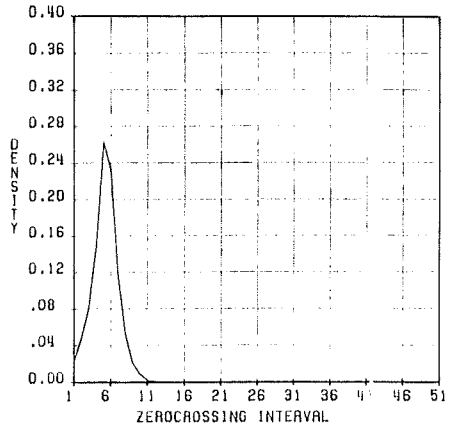

Speaker 4

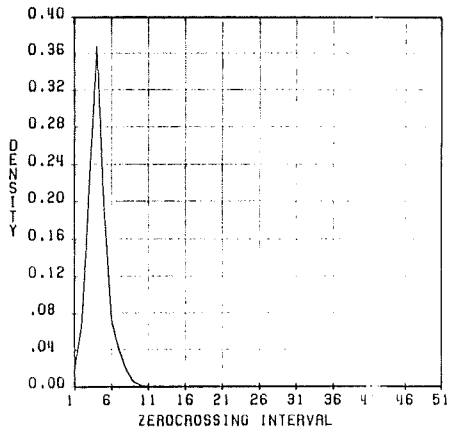

Speaker 5

FIGURE 13. Density functions for the time between zerocrossings for /ch/-sounds.

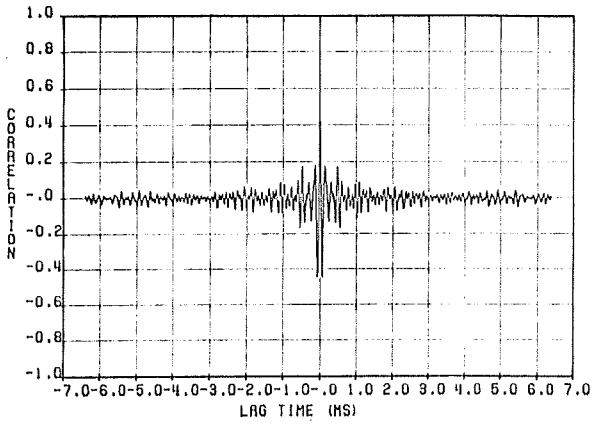

Speaker 1

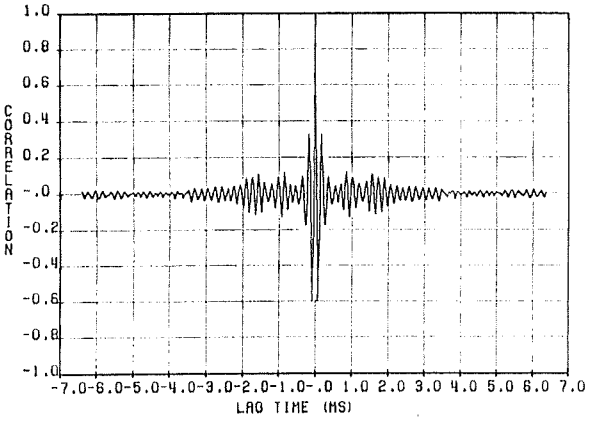

Speaker 2

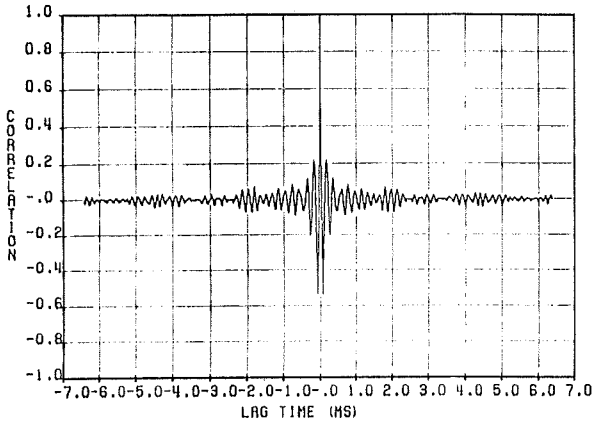

Speaker 3

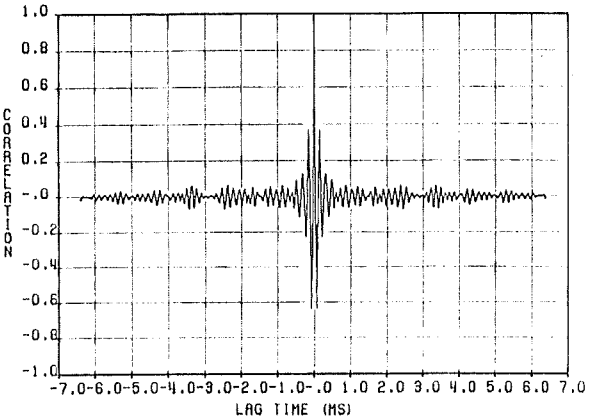

Speaker 4

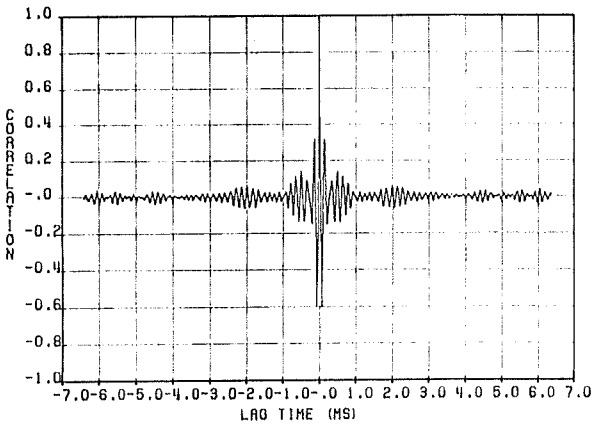

Speaker 5

FIGURE 14. Autocorrelation functions for peak-clipped /s/-sounds.

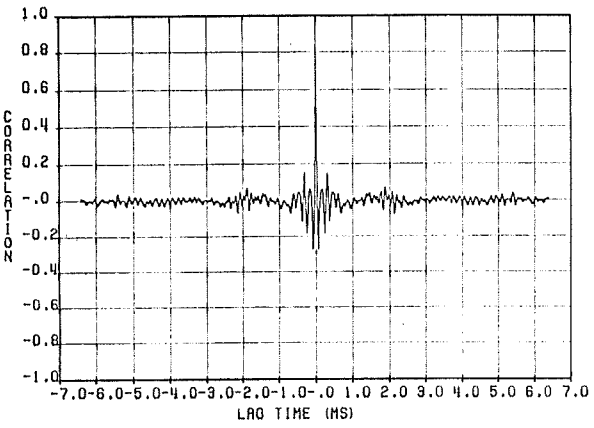

Speaker 1

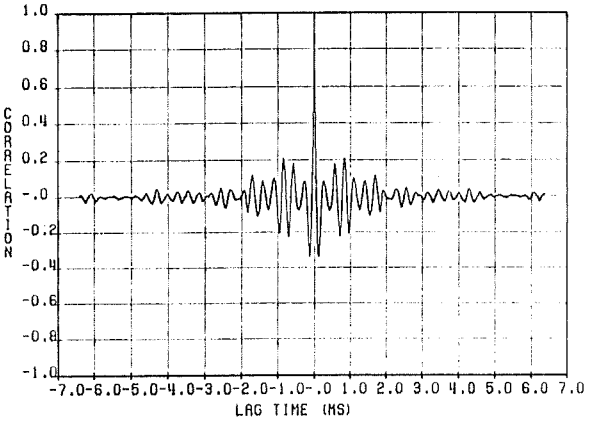

Speaker 2

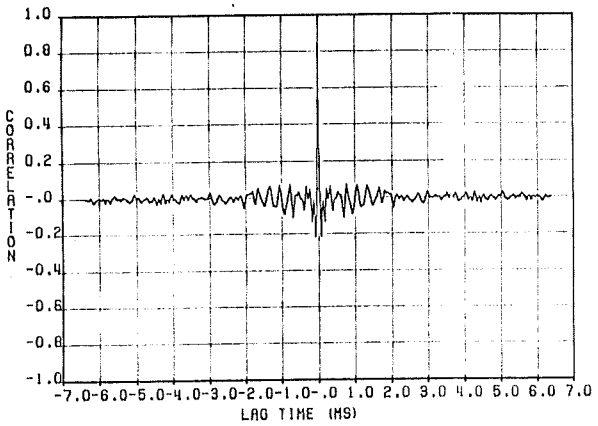

Speaker 3

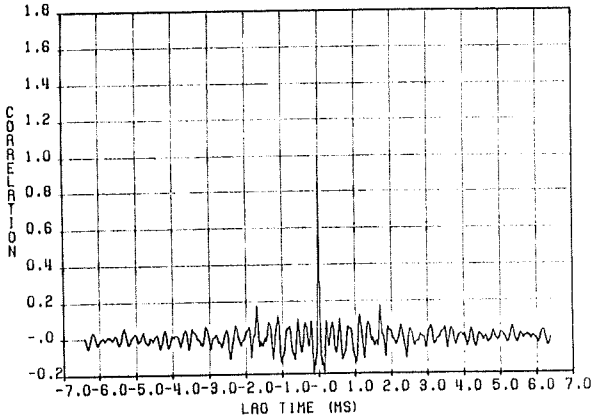

Speaker 4

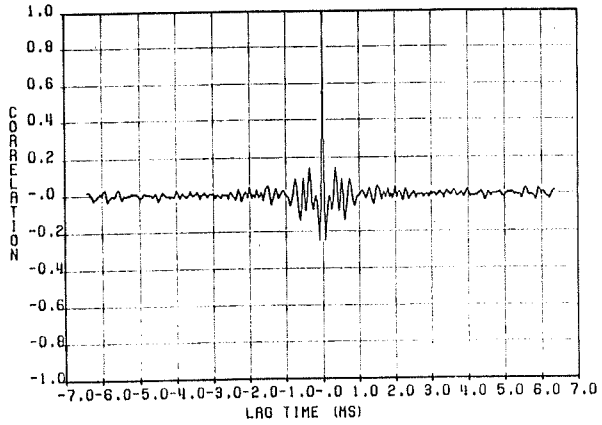

Speaker 5

FIGURE 15. Autocorrelation functions for peak-clipped /f/-sounds.

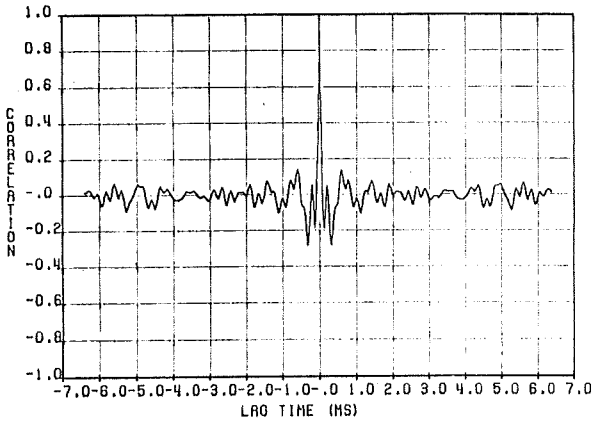

Speaker 1

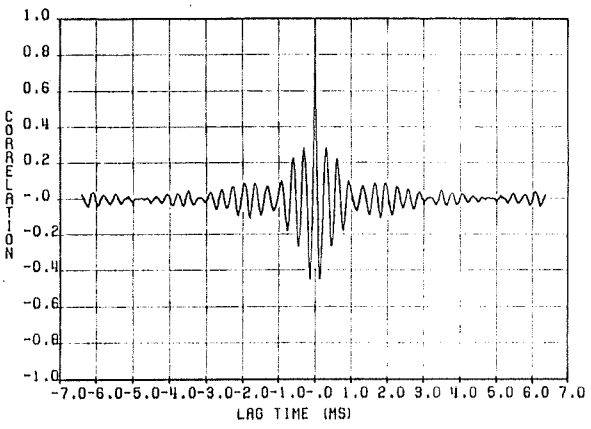

Speaker 2

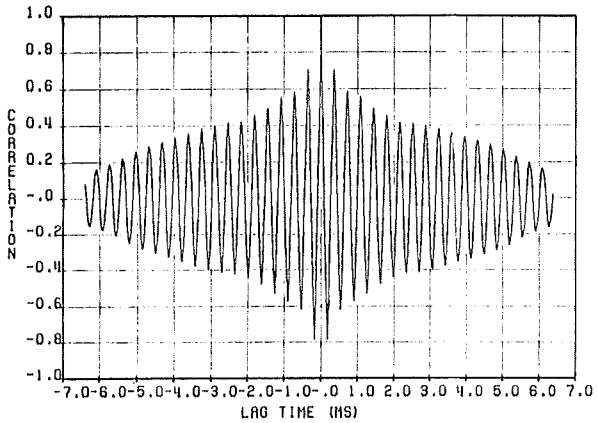

Speaker 3

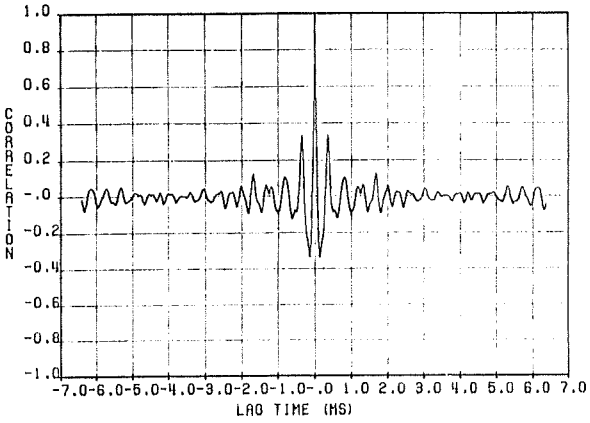

Speaker 4

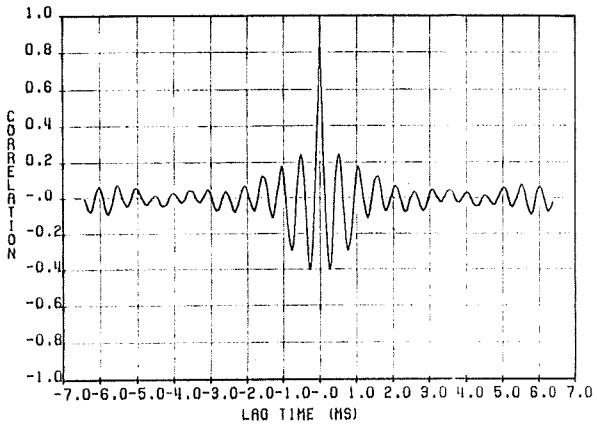

Speaker 5

FIGURE 16. Autocorrelation functions for peak-clipped /sh/-sounds.

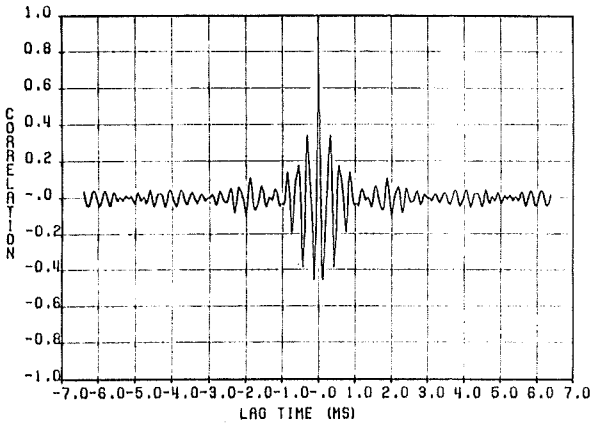

Speaker 1

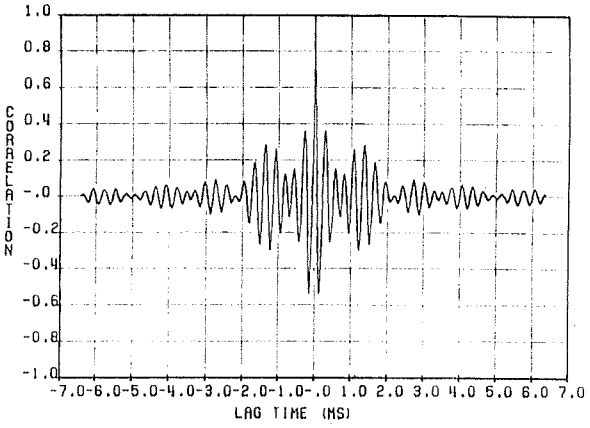

Speaker 2

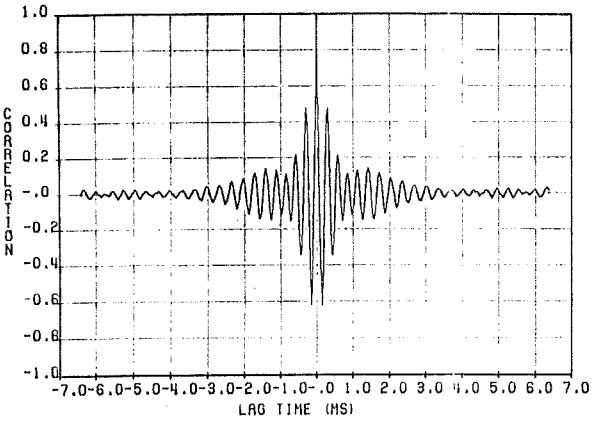

Speaker 3

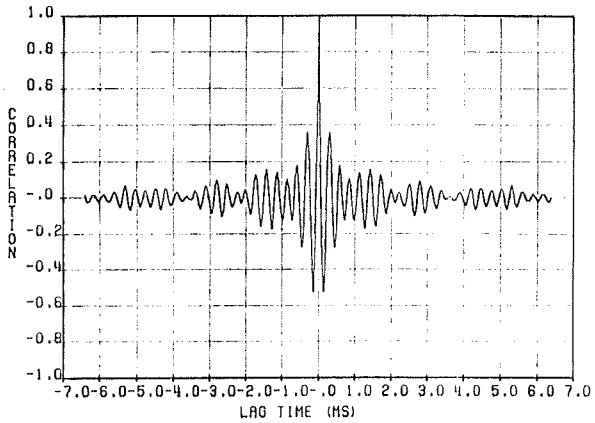

Speaker 4

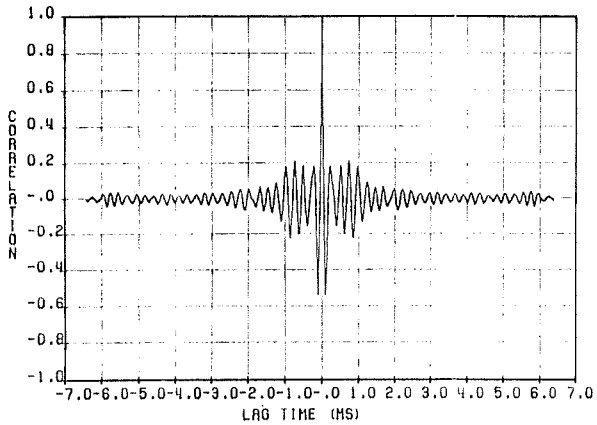

Speaker 5

FIGURE 17. Autocorrelation functions for peak-clipped /ch/-sounds.

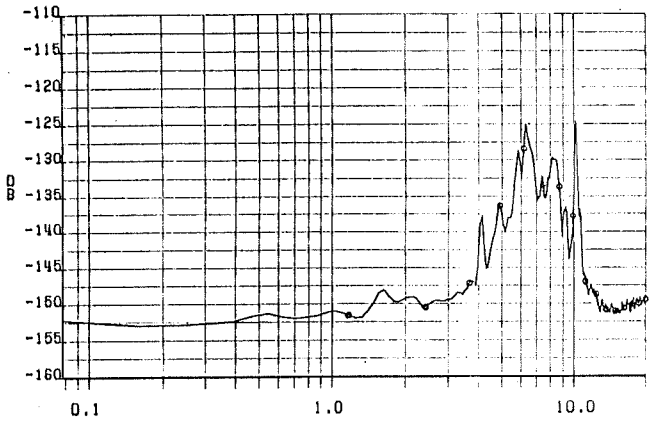

Speaker 1

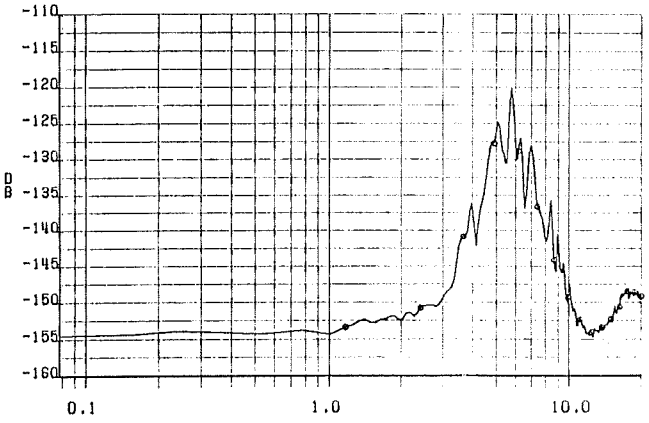

Speaker 2

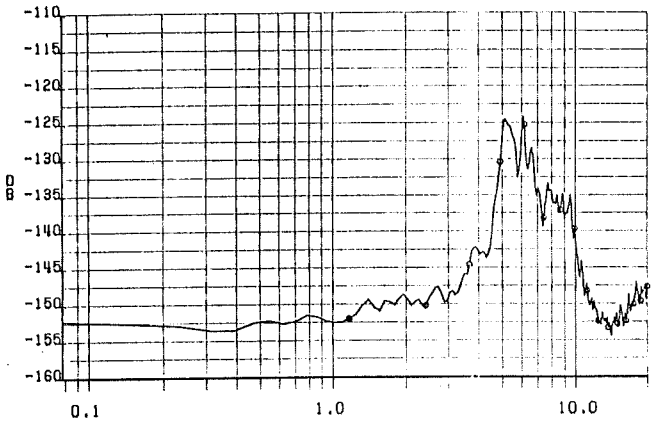

Speaker 3

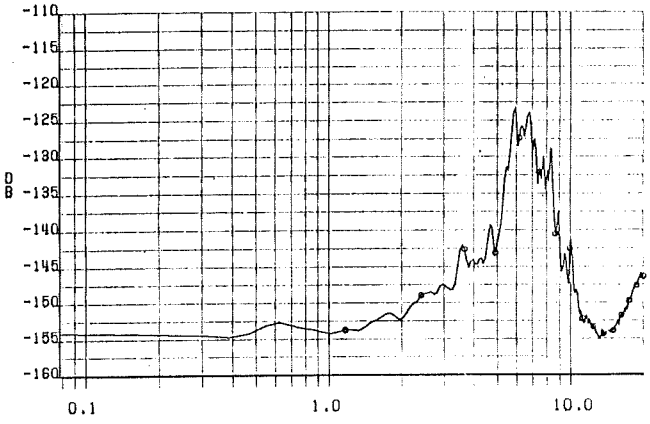

Speaker 4

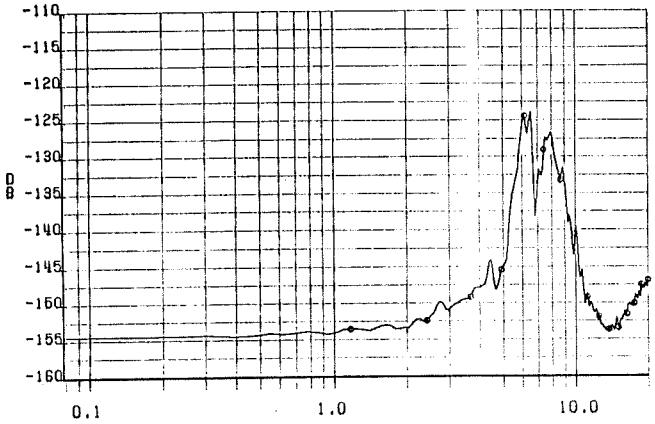

Speaker 5

FIGURE 18. Power spectral density functions for peak-clipped /s/-sounds.

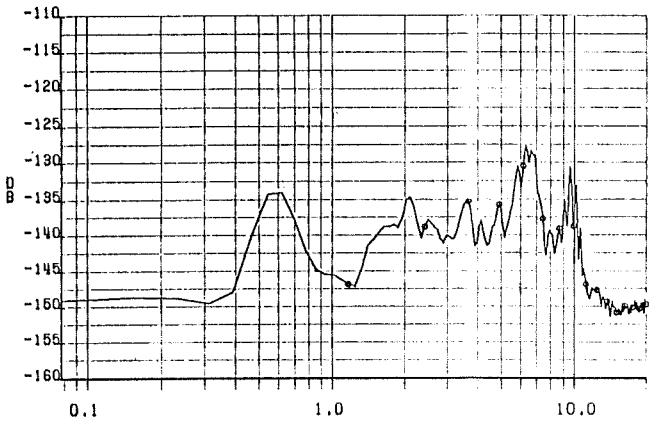

Speaker 1

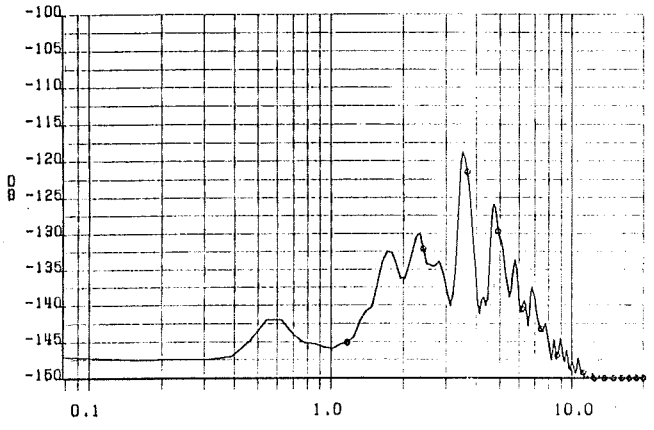

Speaker 2

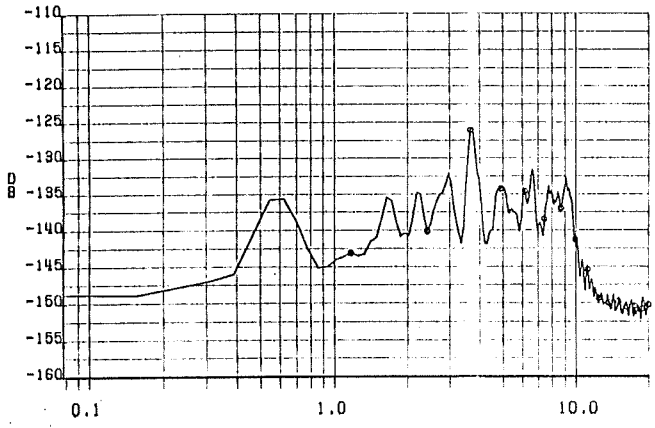

Speaker 3

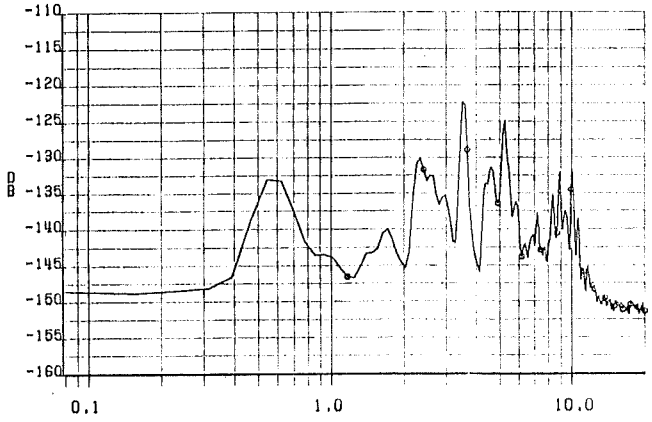

Speaker 4

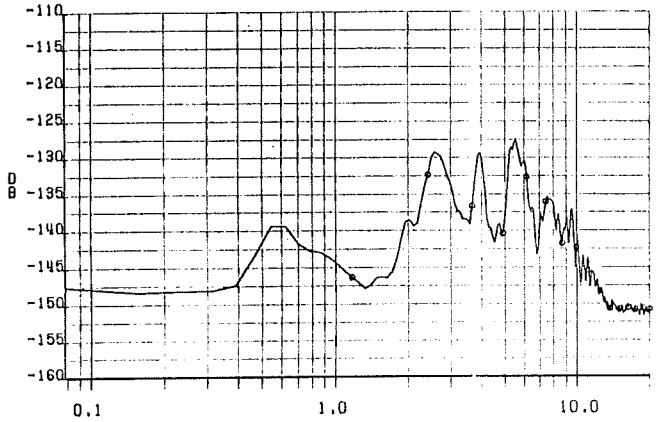

Speaker 5

FIGURE 19. Power spectral density functions for peak-clipped /f/-sounds.

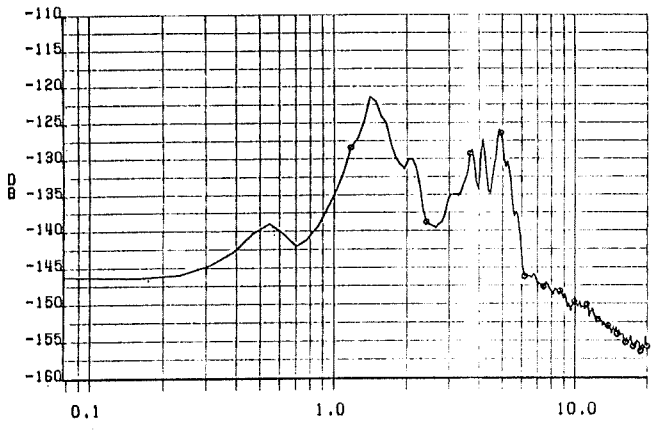

Speaker 1

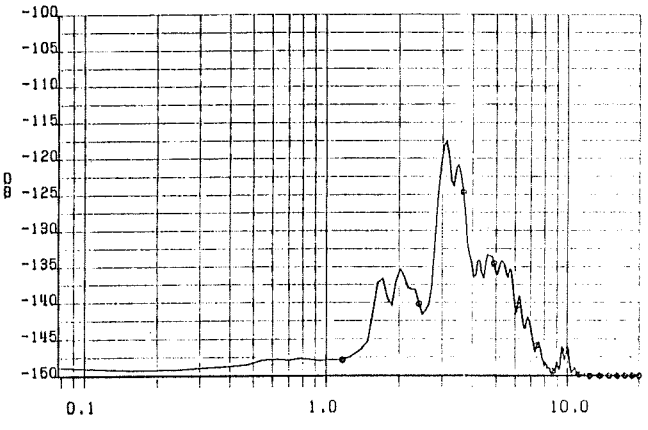

Speaker 2

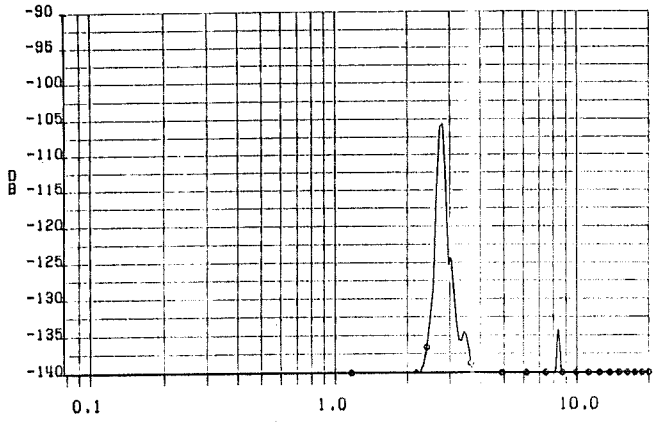

Speaker 3

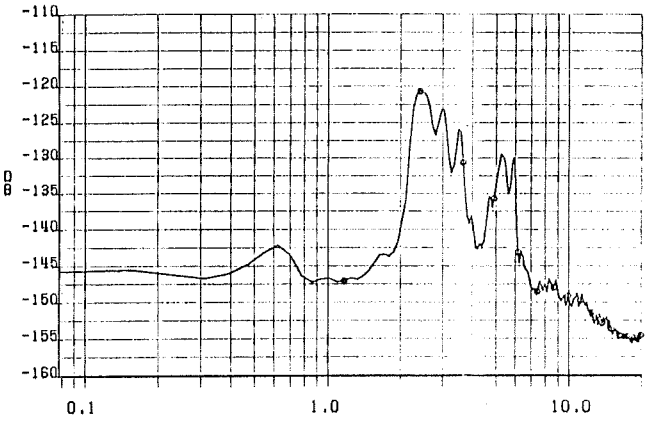

Speaker 4

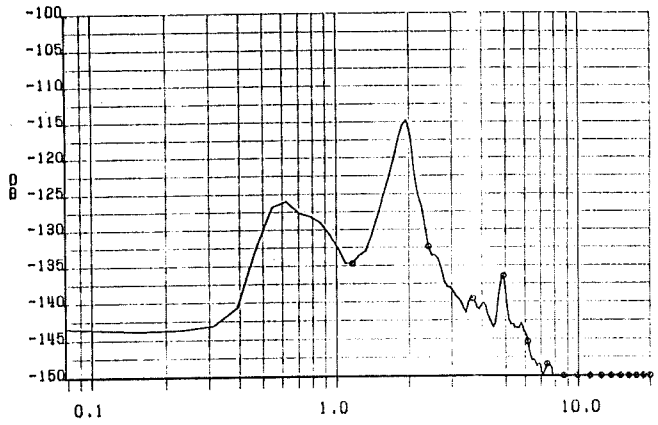

Speaker 5

FIGURE 20. Power spectral density functions for peak-clipped /sh/-sounds.

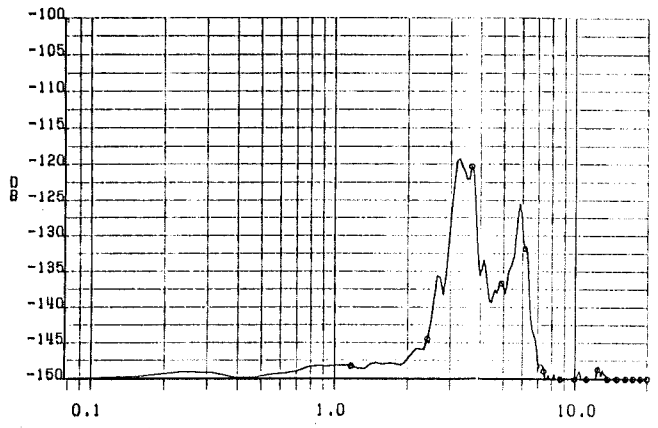

Speaker 1

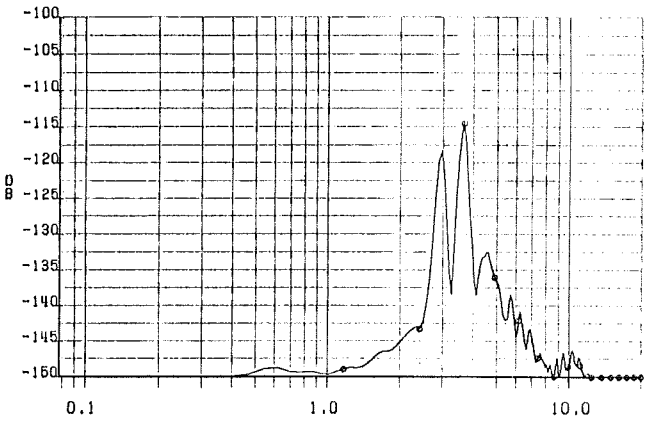

Speaker 2

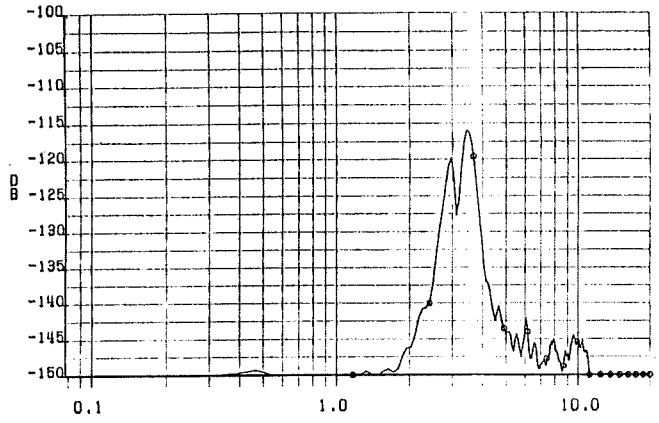

Speaker 3

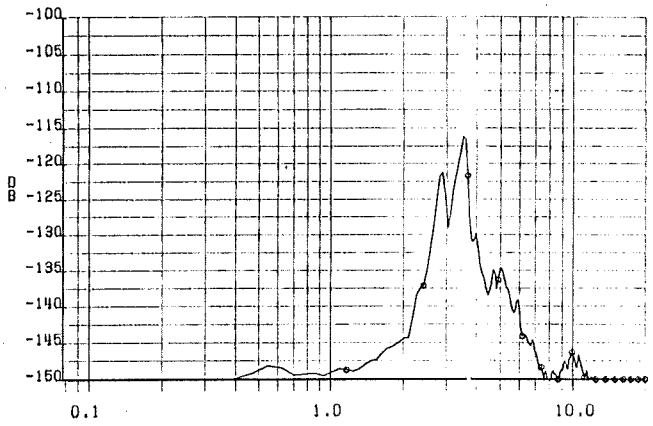

Speaker 4

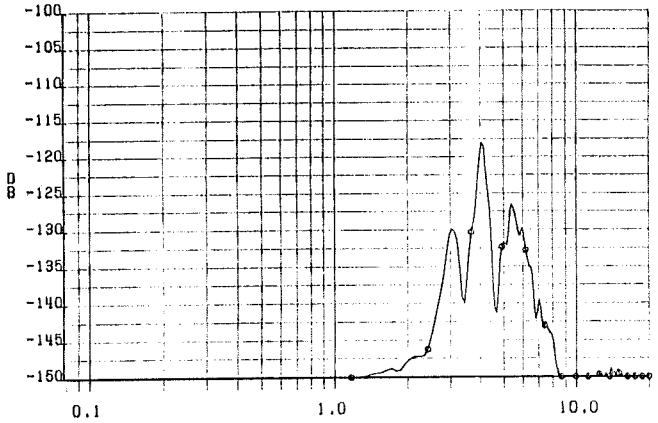

Speaker 5

FIGURE 21. Power spectral density functions for peak-clipped /ch/-sounds.

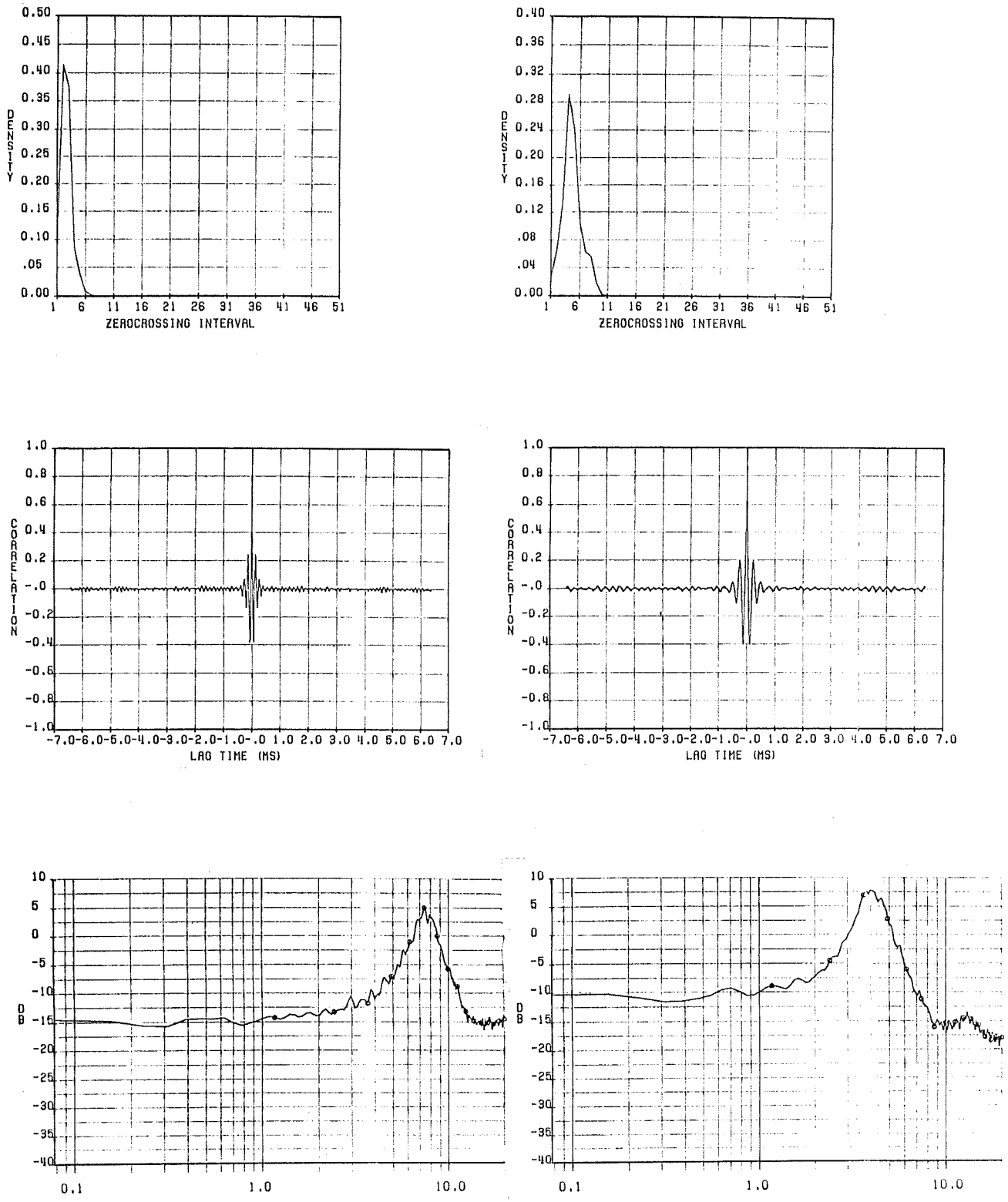

FIGURE 22. Zerocrossing density function, autocorrelation function and spectrum for synthetic /s/-sound (left) and synthetic /ch/-sound (right). The sounds are synthesized from the zerocrossing densities of speaker 1.

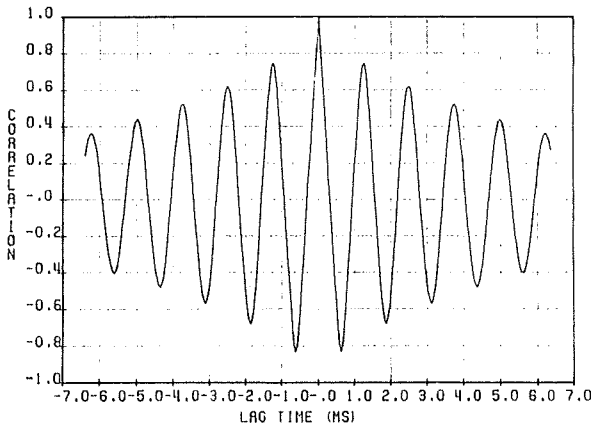

Speaker 1

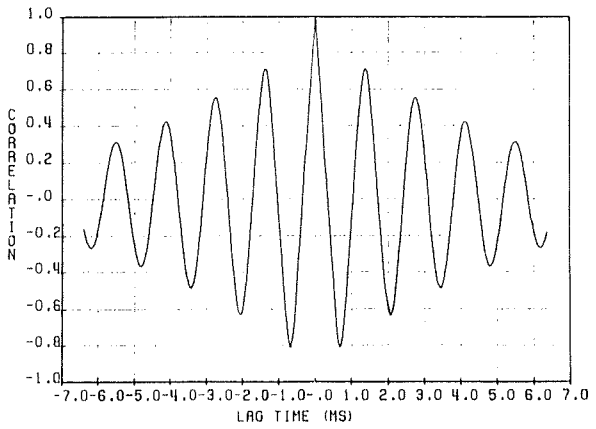

Speaker 2

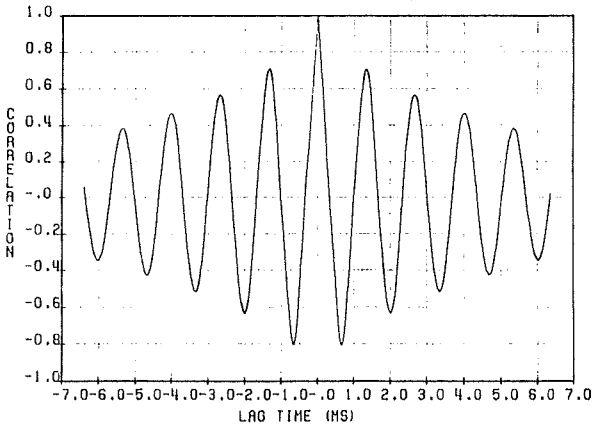

Speaker 3

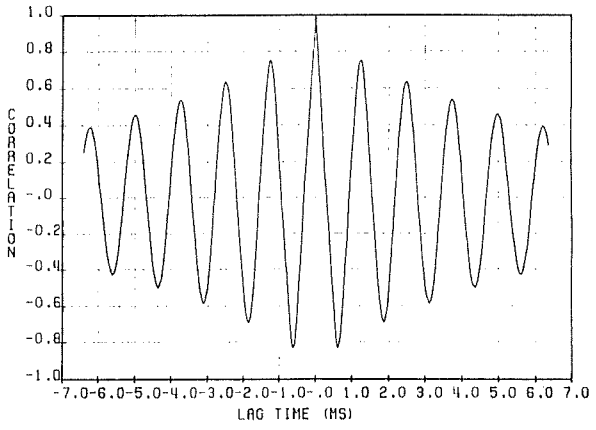

Speaker 4

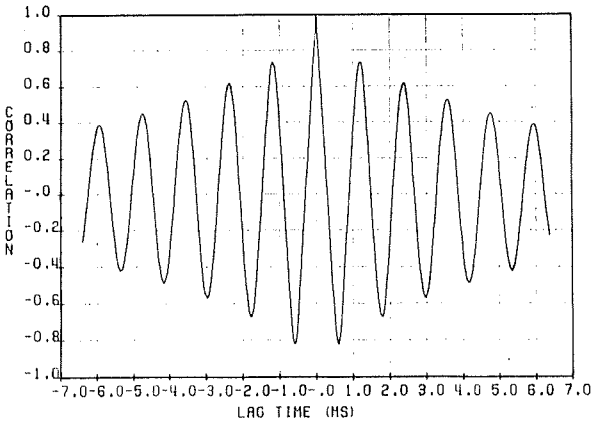

Speaker 5

FIGURE 23. Autocorrelation functions for frequency divided /s/-sounds.

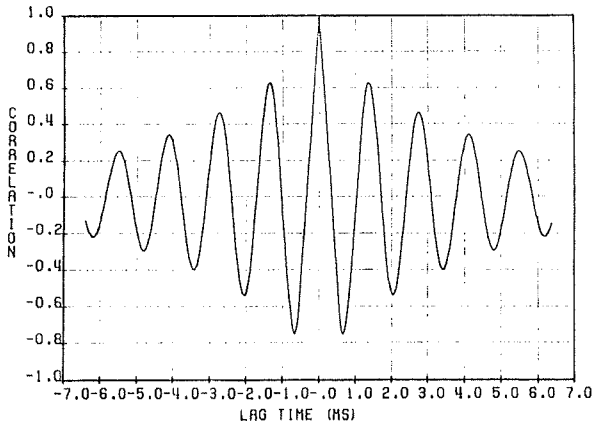

Speaker 1

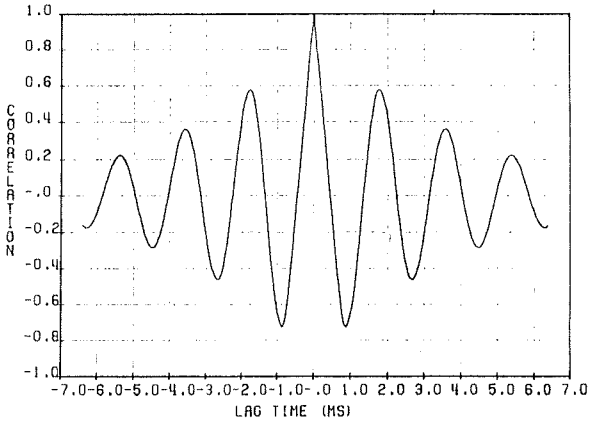

Speaker 2

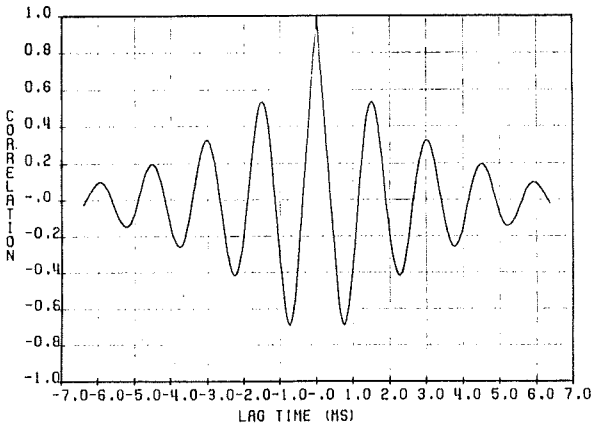

Speaker 3

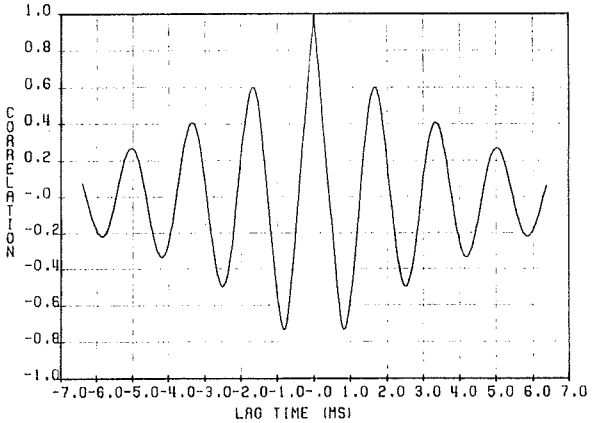

Speaker 4

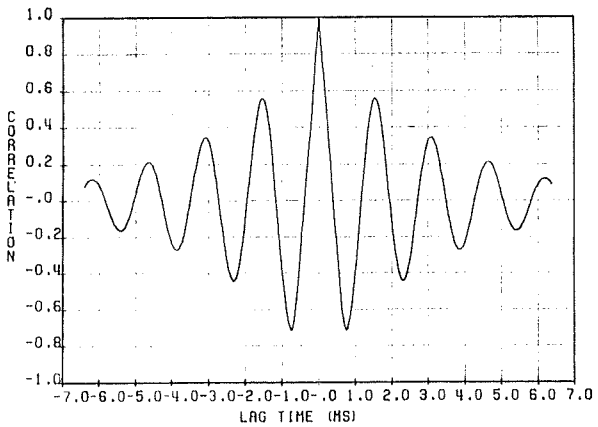

Speaker 5

FIGURE 24. Autocorrelation functions for frequency divided /f/-sounds.

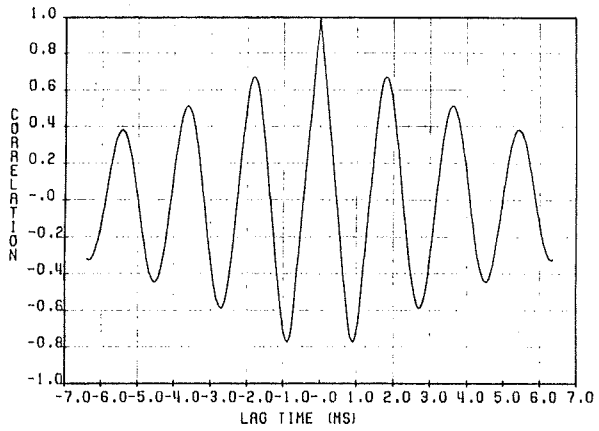

Speaker 1

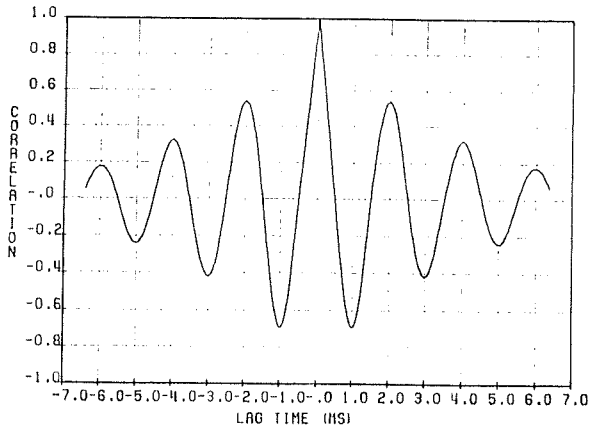

Speaker 2

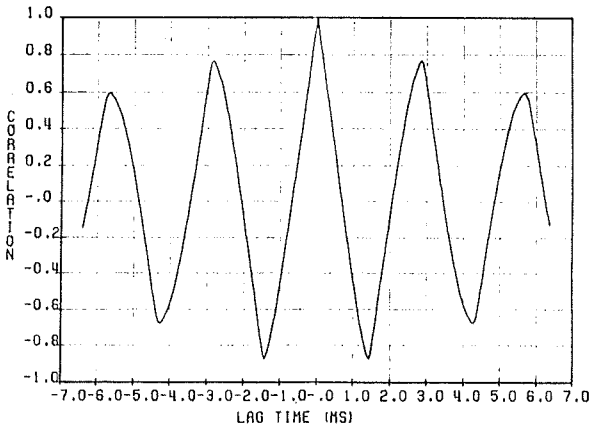

Speaker 3

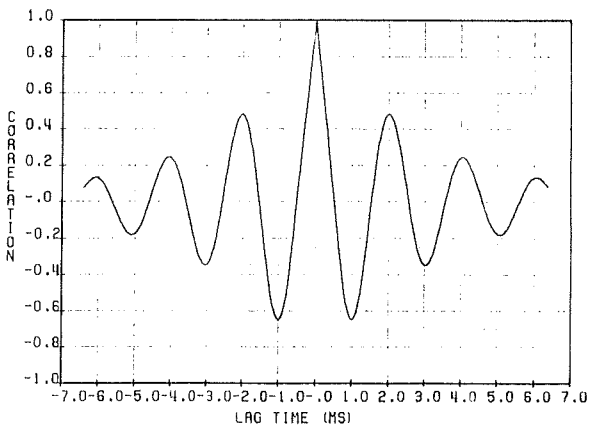

Speaker 4

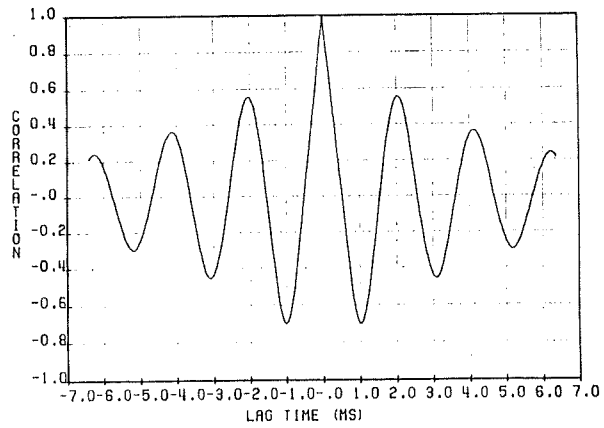

Speaker 5

FIGURE 25. Autocorrelation functions for frequency divided /sh/-sounds.

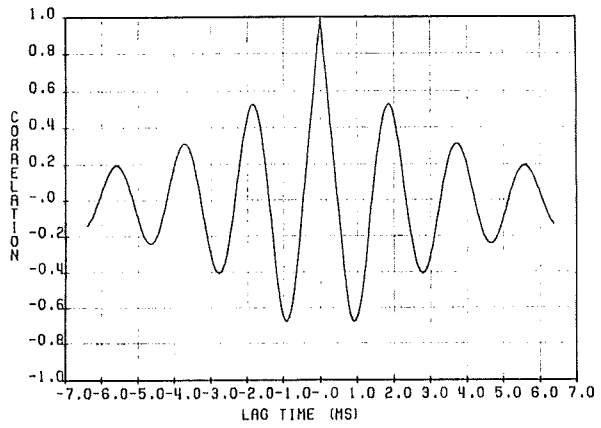

Speaker 1

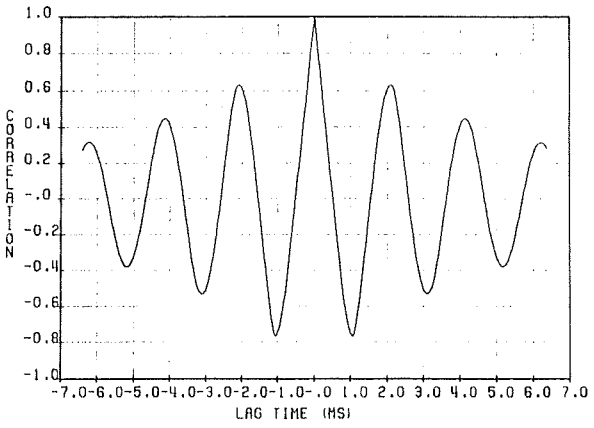

Speaker 2

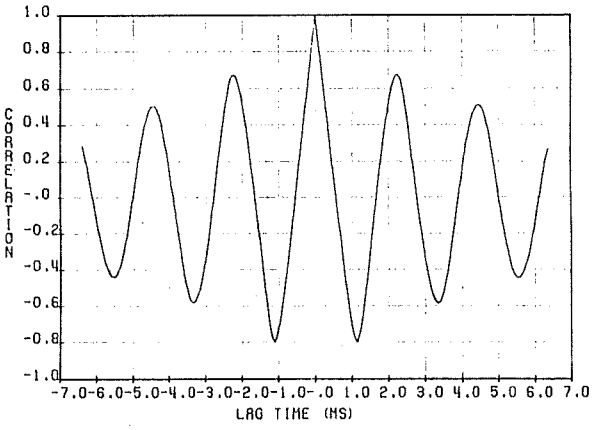

Speaker 3

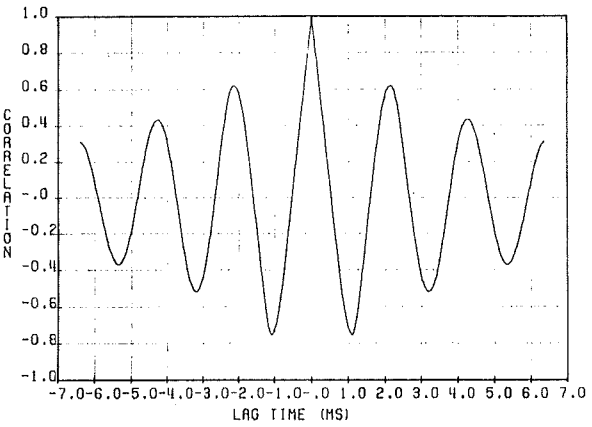

Speaker 4

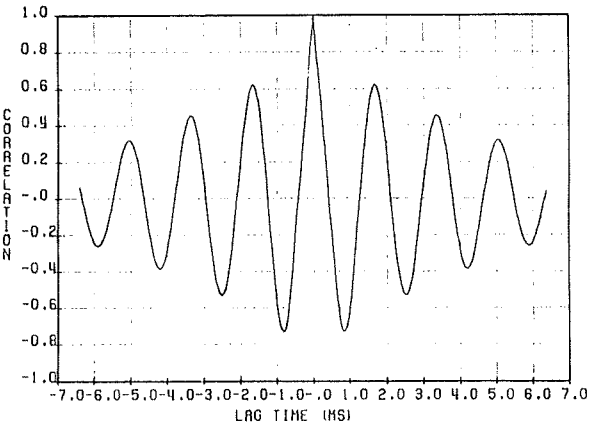

Speaker 5

FIGURE 26. Autocorrelation functions for frequency divided /ch/-sounds.

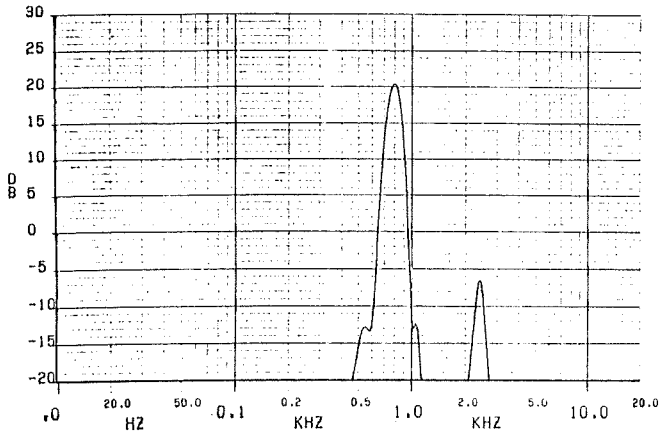

Speaker 1

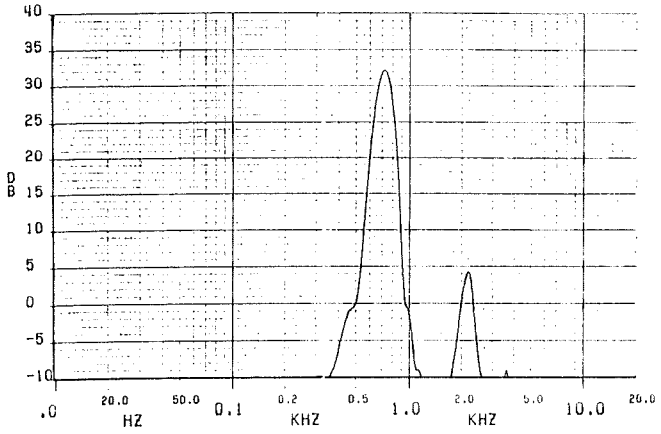

Speaker 2

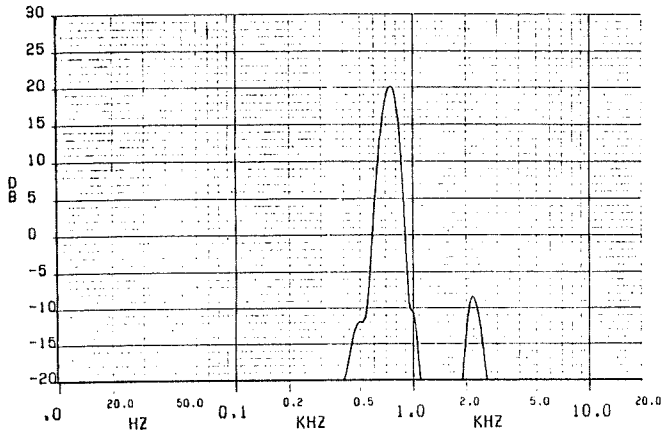

Speaker 3

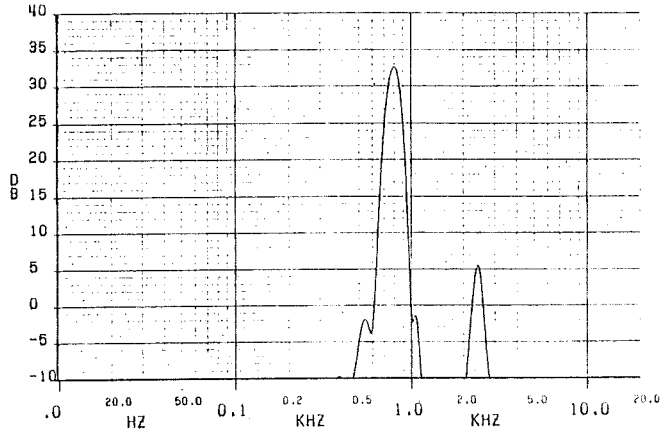

Speaker 4

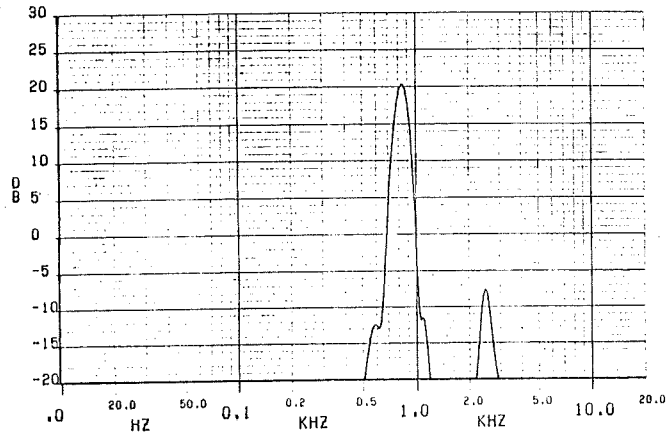

Speaker 5

FIGURE 27. Power spectral density functions for frequency divided /s/-sounds.

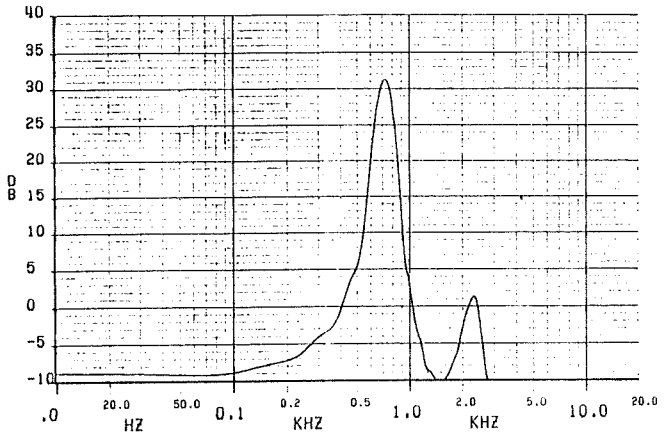

Speaker 1

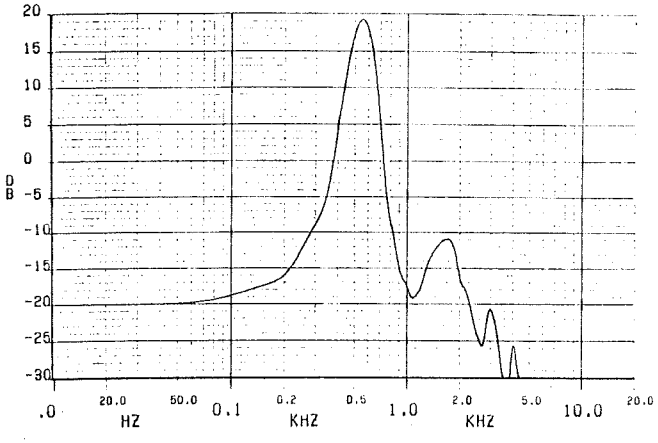

Speaker 2

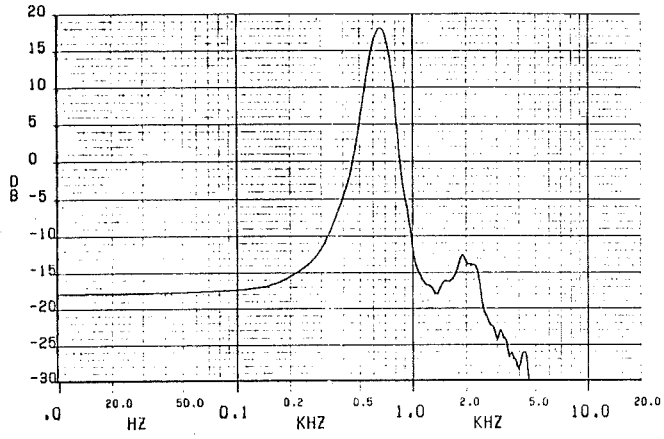

Speaker 3

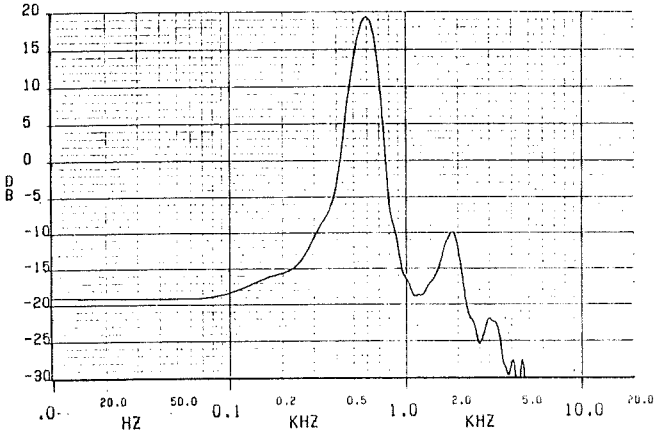

Speaker 4

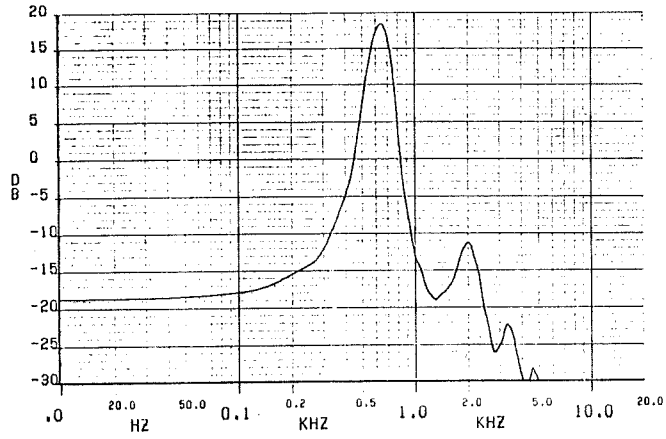

Speaker 5

FIGURE 28. Power spectral density functions for frequency divided /f/-sounds.

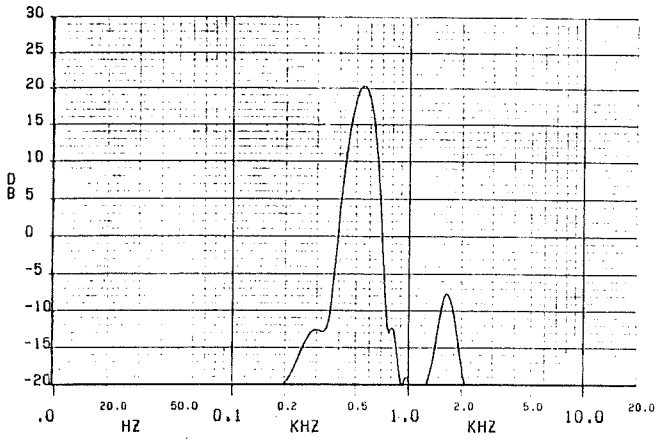

Speaker 1

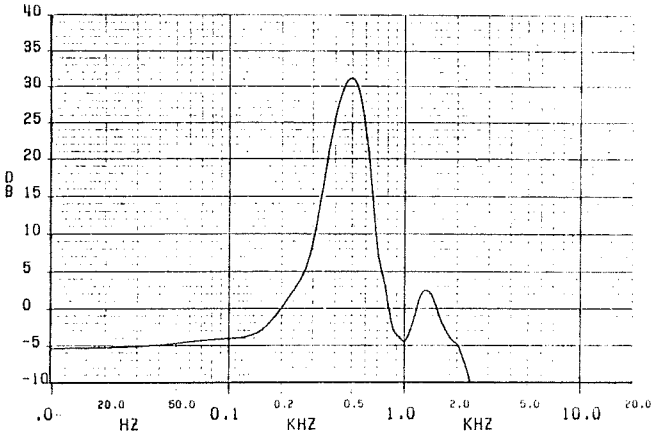

Speaker 2

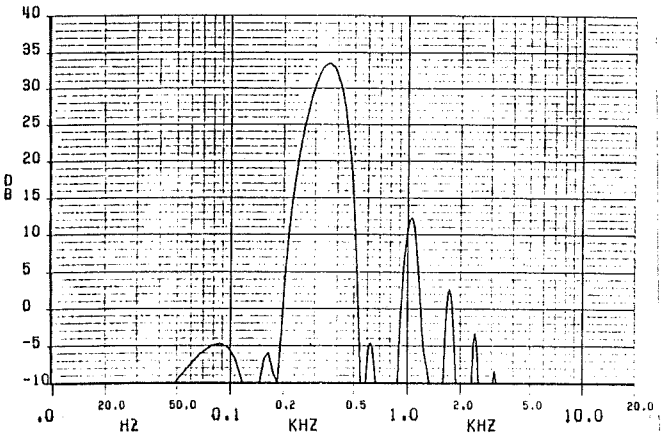

Speaker 3

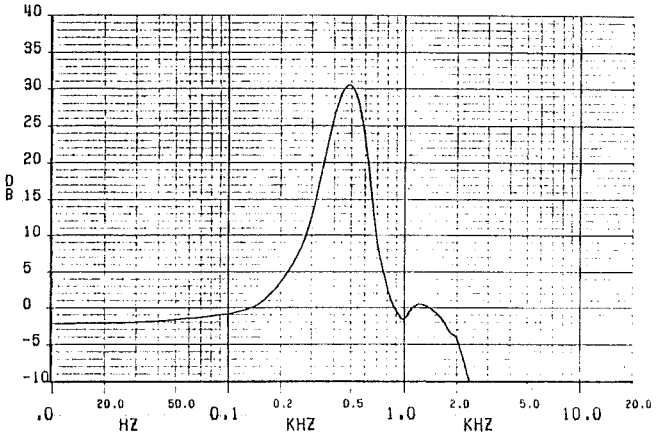

Speaker 4

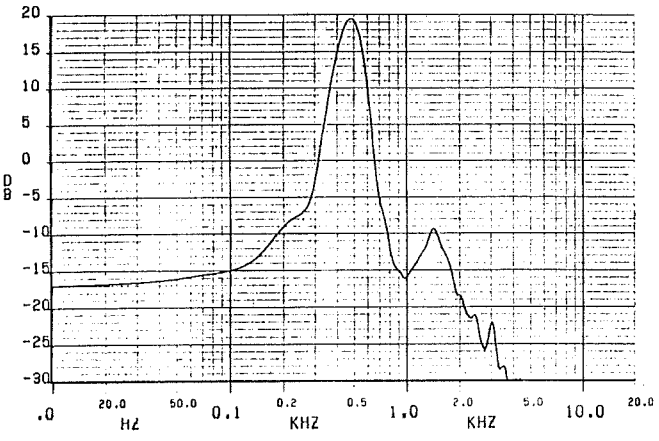

Speaker 5

FIGURE 29. Power spectral density functions for frequency divided /sh/-sounds.

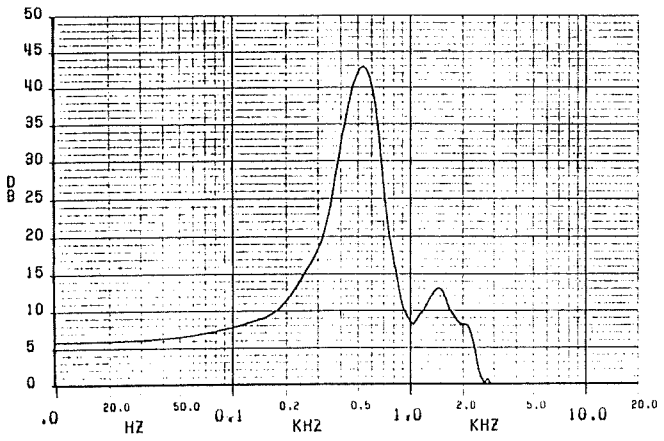

Speaker 1

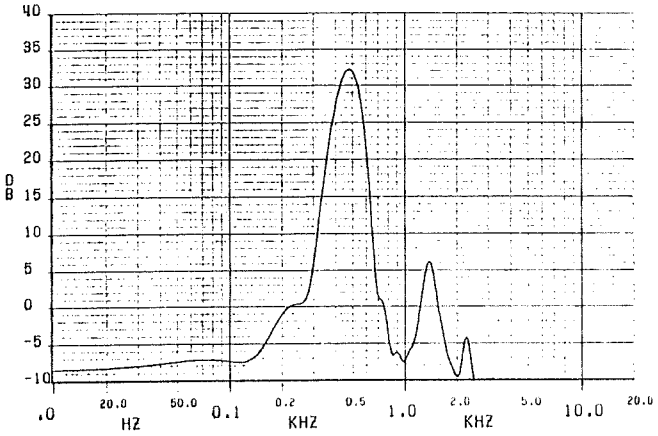

Speaker 2

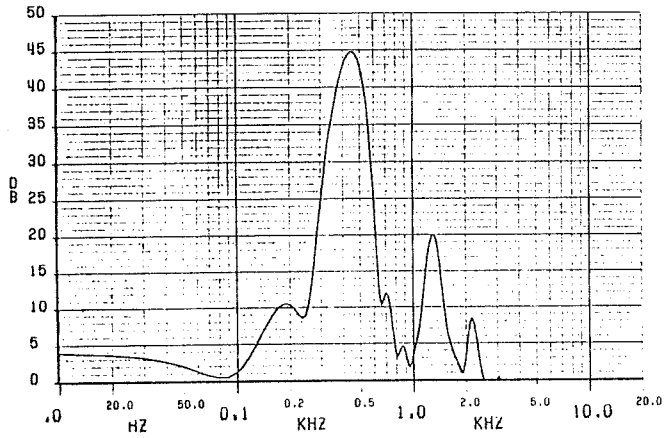

Speaker 3

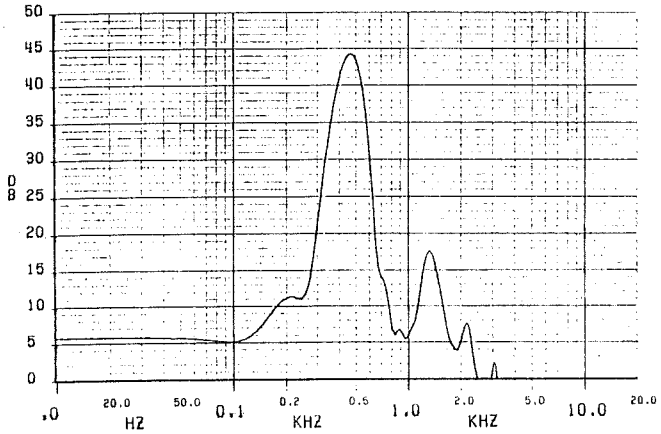

Speaker 4

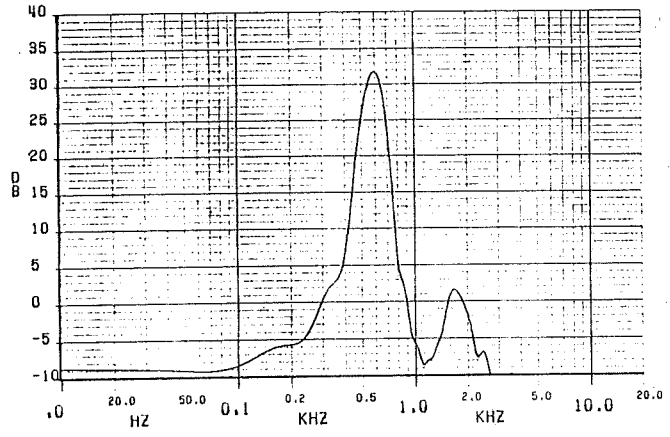

Speaker 5

FIGURE 30. Power spectral density functions for frequency divided /ch/-sounds.